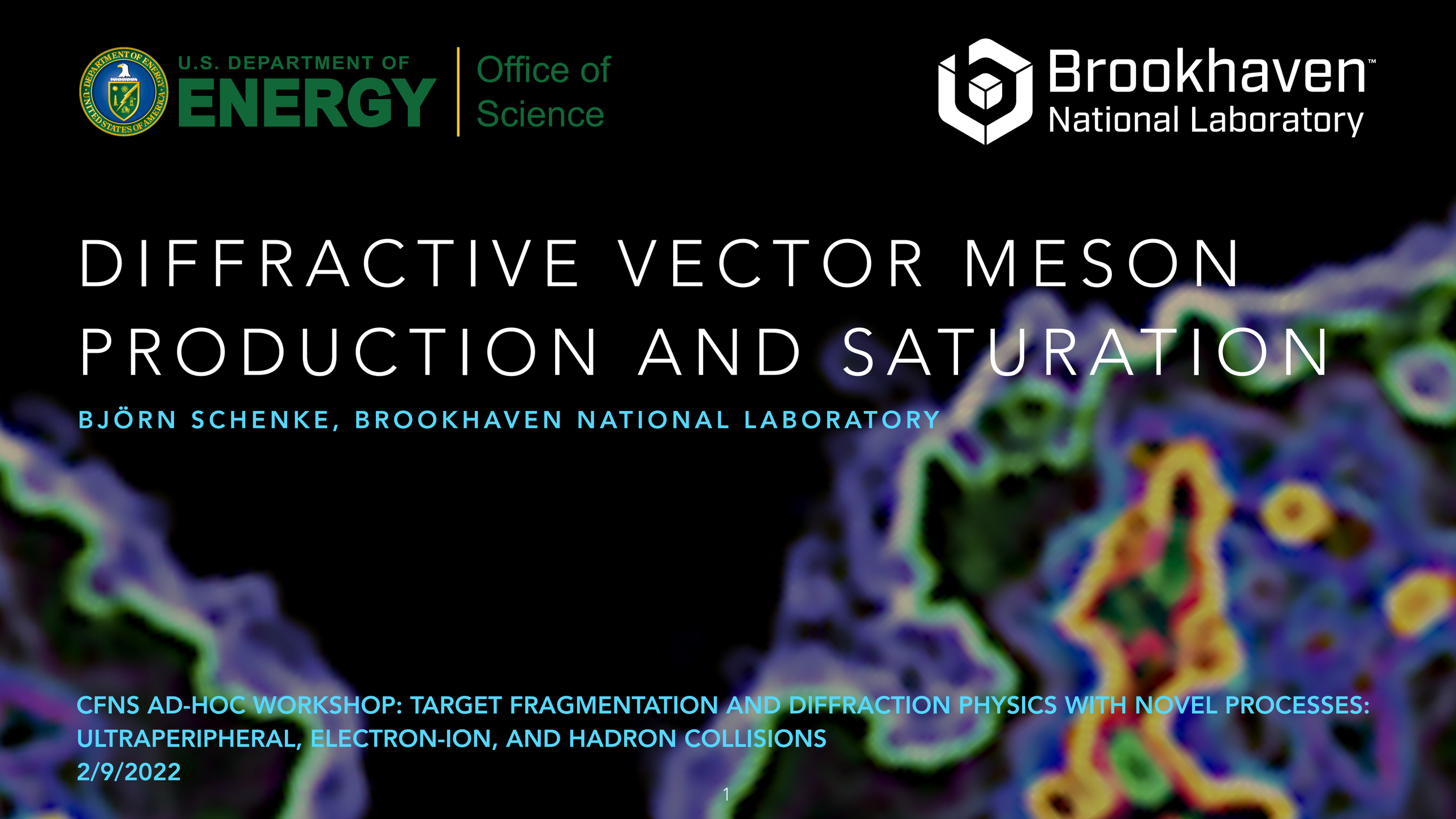

U.S. DEPARTMENT OF ENERGY | Office of Science

Brookhaven National Laboratory

DIFFRACTIVE VECTOR MESON PRODUCTION AND SATURATION

BJÖRN SCHENKE, BROOKHAVEN NATIONAL LABORATORY

CFNS AD-HOC WORKSHOP: TARGET FRAGMENTATION AND DIFFRACTION PHYSICS WITH NOVEL PROCESSES: ULTRAPERIPHERAL, ELECTRON-ION, AND HADRON COLLISIONS
2/9/2022

Diffractive vector meson production

- Diffractive processes can constrain the average shape of the target and probe event-by-event fluctuations at different distance scales

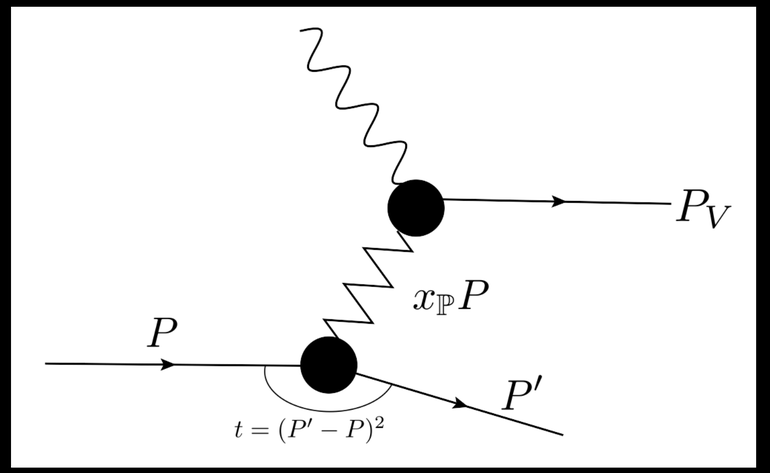

- High energy: Use dipole picture and color glass condensate to describe the target

- Saturation effects show up in e.g. Q^2 dependence and $|t|$ spectra

Coherent diffraction:

Target remains in the same quantum state after the interaction

Apply Good-Walker formalism: Cross section is determined by the average interaction of the states that diagonalize the scattering matrix with the target. M. L. Good and W. D. Walker, Phys. Rev. 120 (1960) 1857

High energy: Fock states of the incoming virtual photon with a fixed number of partons (LO: quark-antiquark pair) at fixed transverse coordinates, probing a fixed configuration of the target.

$$\frac{d\sigma^{\gamma^* A \to VA}}{dt} = \frac{1}{16\pi} \left| \left\langle \mathcal{A}^{\gamma^* A \to VA} \right\rangle \right|^2$$

Incoherent diffraction:

Initial state: $|i\rangle$; Final state: $|f\rangle$; Amplitude for diffractive scattering: $\mathcal{A}$

Squared transition amplitude, which enters in the cross section:

H. I. Miettinen and J. Pumplin, Phys. Rev. D18 (1978) 1696

$$\sum_{f\neq i} |\langle f|\mathcal{A}|i\rangle|^2 = \sum_{f} \langle i|\mathcal{A}^*|f\rangle\langle f|\mathcal{A}|i\rangle - \langle i|\mathcal{A}|i\rangle\langle i|\mathcal{A}^*|i\rangle$$

$$= \langle i|\mathcal{A}^*\mathcal{A}|i\rangle - |\langle i|\mathcal{A}|i\rangle|^2$$

Sum over final states includes all possible states for the final state target

Average over all possible initial states → cross section

$$\frac{d\sigma^{\gamma^* A\to VA}}{dt} = \frac{1}{16\pi}\left(\left\langle\left|\mathcal{A}^{\gamma^* A\to VA}\right|^2\right\rangle - \left|\left\langle\mathcal{A}^{\gamma^* A\to VA}\right\rangle\right|^2\right)$$

Dipole picture: Scattering amplitude

H. Mäntysaari, B. Schenke, Phys. Rev. Lett. 117 (2016) 052301; Phys.Rev. D94 (2016) 034042

High energy factorization:

- $\gamma^* \to q\bar{q} : \psi^{\gamma}(r, Q^2, z)$
- $q\bar{q}$ dipole scatters with amplitude N
- $q\bar{q} \to V : \psi^{V}(r, Q^2, z)$

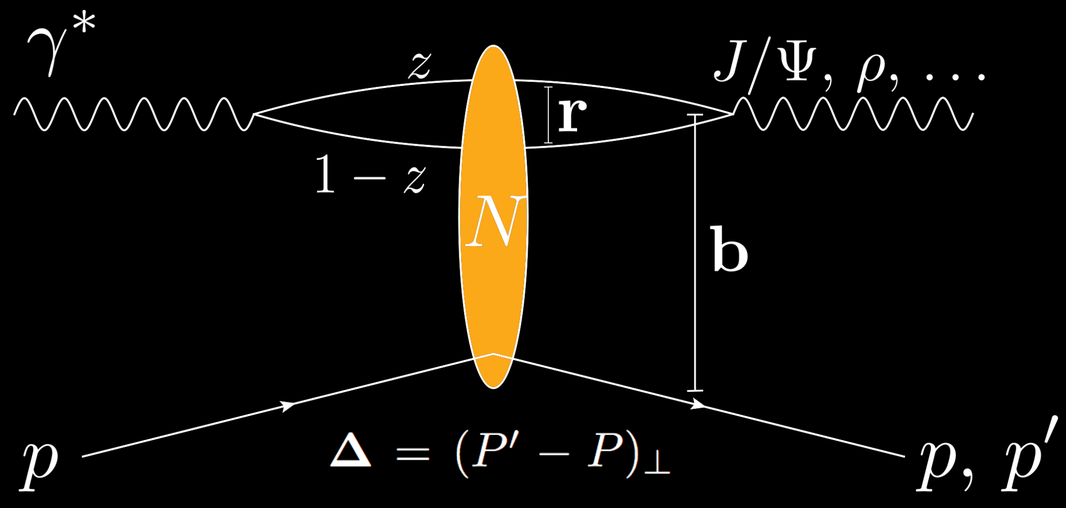

$$\mathcal{A} \sim \int \mathrm{d}^2 b \mathrm{d} z \mathrm{d}^2 r \Psi^* \Psi^V(r, z, Q^2) e^{-ib\cdot\Delta} N(r, x, b)$$

- Impact parameter ***b*** is the Fourier conjugate of transverse momentum transfer ***Δ*** → Access spatial structure ($t = -\Delta^2$)
- Total F_2: forward scattering amplitude (***Δ***=0) for V=γ (same N)

Modeling the dipole amplitude

H. Mäntysaari, B. Schenke, Phys. Rev. Lett. 117 (2016) 052301; Phys.Rev. D94 (2016) 034042

One way: IPSat model:

$$N = 1 - \exp[-r^2 F(x, r^2) T(\vec{b})] \quad \text{with} \quad F(x, \vec{r}^2) = \frac{\pi^2}{2N_c} \alpha_s \left(\mu_0^2 + \frac{C}{r^2}\right) xg\left(x, \mu_0^2 + \frac{C}{r^2}\right)$$

Proton targets: parameters $\mu_0^2, C, xg(x, \mu_0^2), B_{\mathrm{p}}$(in T) constrained by HERA data; Scale dependence of xg obtained from DGLAP evolution

Two models for the proton shape …

Modeling the dipole amplitude

H. Mäntysaari, B. Schenke, Phys. Rev. Lett. 117 (2016) 052301; Phys.Rev. D94 (2016) 034042

1) Assume Gaussian proton shape:

$$T(\vec{b}) = T_{\mathrm{p}}(\vec{b}) = \frac{1}{2\pi B_{\mathrm{p}}} e^{-b^2/(2B_{\mathrm{p}})}$$

2) Assume Gaussian distributed and Gaussian shaped hot spots:

$$P(b_i) = \frac{1}{2\pi B_{\mathrm{qc}}} e^{-b_i^2/(2B_{\mathrm{qc}})}$$ (angles uniformly distributed)

$$T_{\mathrm{p}}(\vec{b}) = \frac{1}{N_{\mathrm{q}}} \sum_{i=1}^{N_{\mathrm{q}}} T_{\mathrm{q}}(\vec{b} - \vec{b}_i)$$ with N_{q}=3 hot spots; $$T_{\mathrm{q}}(\vec{b}) = \frac{1}{2\pi B_{\mathrm{q}}} e^{-b^2/(2B_{\mathrm{q}})}$$

Results compared to HERA data

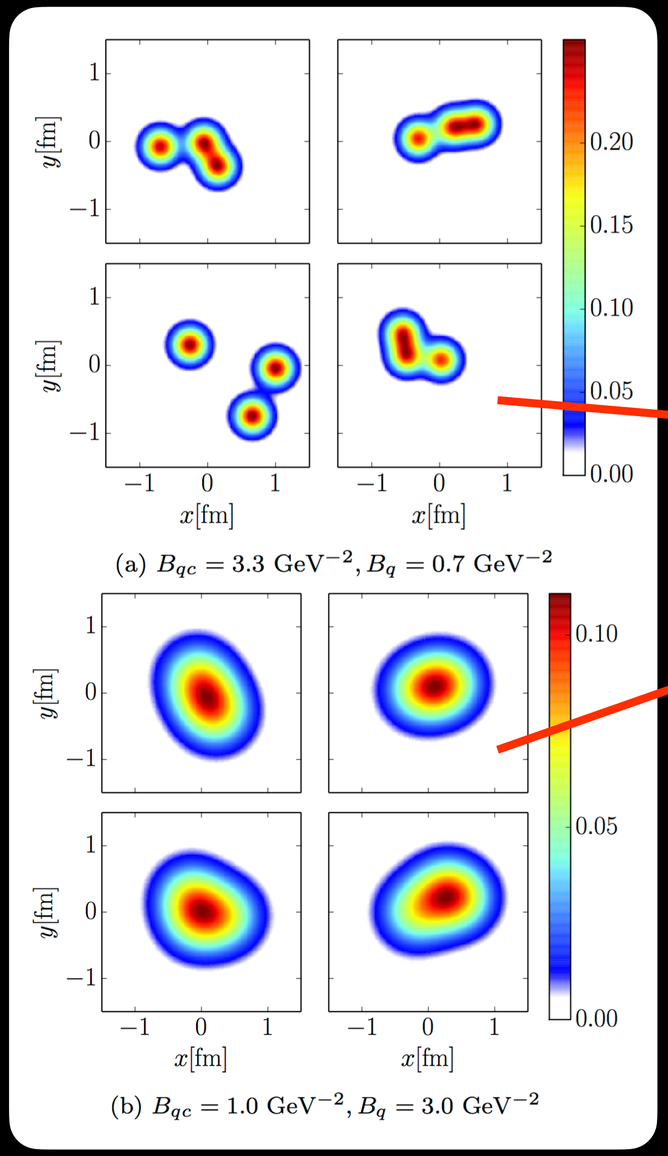

H. Mäntysaari, B. Schenke, Phys. Rev. Lett. 117 (2016) 052301
Phys.Rev. D94 (2016) 034042

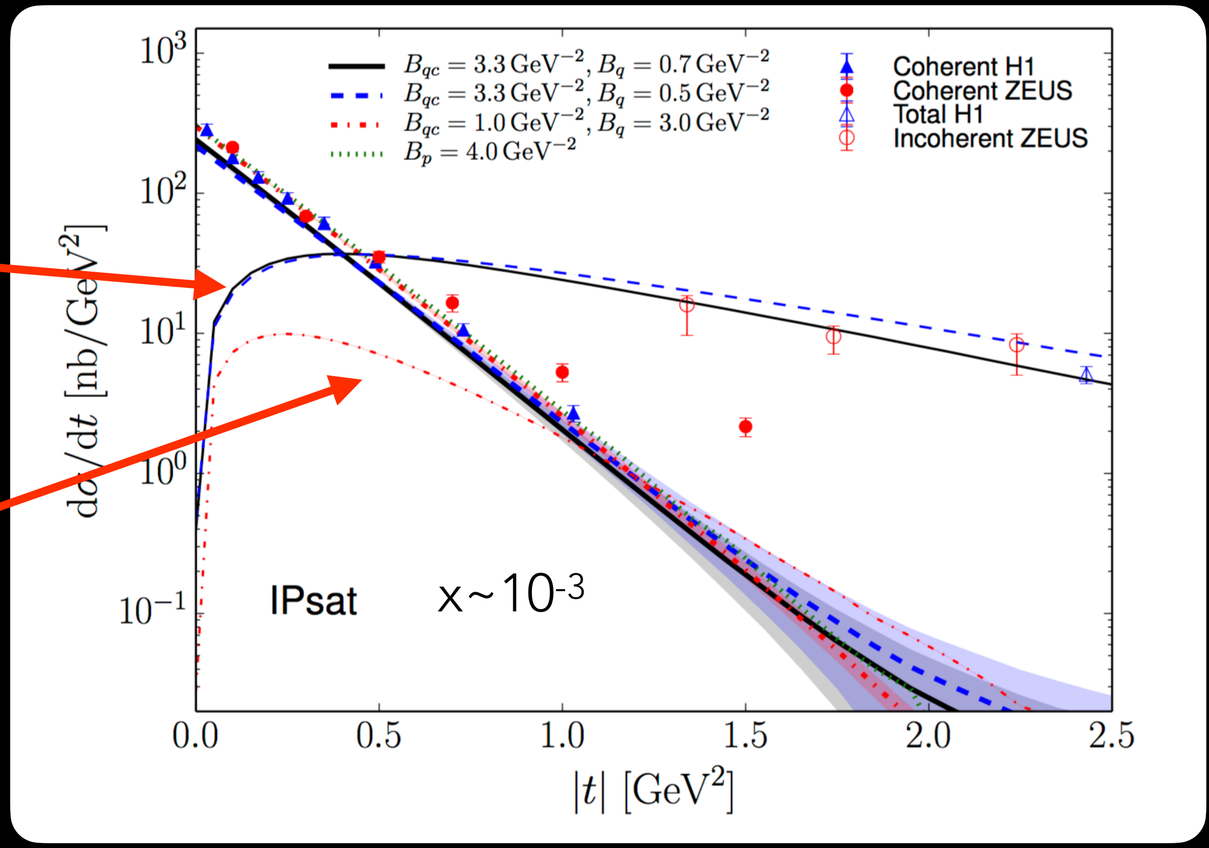

H1 collaboration, Eur. Phys. J. C46 (2006) 585, Phys. Lett. B568 (2003) 205
ZEUS collaboration, Eur. Phys. J. C24 (2002) 345, Eur. Phys. J. C26 (2003) 389

Color Glass Condensate formalism

H. Mäntysaari, B. Schenke, Phys.Rev.D 98 (2018) 3, 034013

Besides IPSat we can compute the dipole amplitude from Wilson lines using the MV model and JIMWLK evolution (with the geometry as in IPSat)

Sample (local Gaussian) color charges with zero mean and

$$\langle \rho^a \rho^b \rangle \sim \delta^{ab} \delta^{(2)}(\vec{x} - \vec{y}) \delta(x^- - y^-) Q_s^2(\vec{x})$$

where Q_s at the initial x_0 is obtained from IPSat

MV model: L. D. McLerran and R. Venugopalan, Phys. Rev. D49 (1994) 2233
JIMWLK: J. Jalilian-Marian, A. Kovner, A. Leonidov, and H. Weigert,
Nucl. Phys. B504, 415 (1997), Phys. Rev. D59, 014014 (1999)
E. Iancu, A. Leonidov, and L. D. McLerran, Nucl. Phys. A692, 583 (2001)
E. Ferreiro, E. Iancu, A. Leonidov, and L. McLerran, Nucl. Phys. A703, 489 (2002)
A. H. Mueller, Phys. Lett. B523, 243 (2001)

Color Glass Condensate formalism

H. Mäntysaari, B. Schenke, Phys.Rev.D 98 (2018) 3, 034013

From color charges we obtain Wilson lines at the initial $x_0 = 0.01$

$$V(\vec{x}) = P \exp\left(-ig \int dx^- \frac{\rho(x^-, \vec{x})}{\vec{\nabla}^2 + \tilde{m}^2} \right)$$

from solution of Yang-Mills equations, with regulator $\tilde{m}$

Dipole amplitude: $N(\vec{r}, x_{\mathbb{P}}, \vec{b}) = N(\vec{x} - \vec{y}, x_{\mathbb{P}}, (\vec{x} + \vec{y})/2) = \mathrm{Tr} V(\vec{x}) V^\dagger(\vec{y})/N_c$

Evolution is done using the Langevin formulation of the JIMWLK equations

K. Rummukainen and H. Weigert Nucl. Phys. A739 (2004) 183; T. Lappi, H. Mäntysaari, Eur. Phys. J. C73 (2013) 2307

Long distance tales are tamed by imposing a regulator in the JIMWLK kernel, *m* S. Schlichting, B. Schenke, Phys.Lett. B739 (2014) 313-319

e+p compared to HERA data

H. Mäntysaari, B. Schenke, Phys.Rev.D 98 (2018) 3, 034013

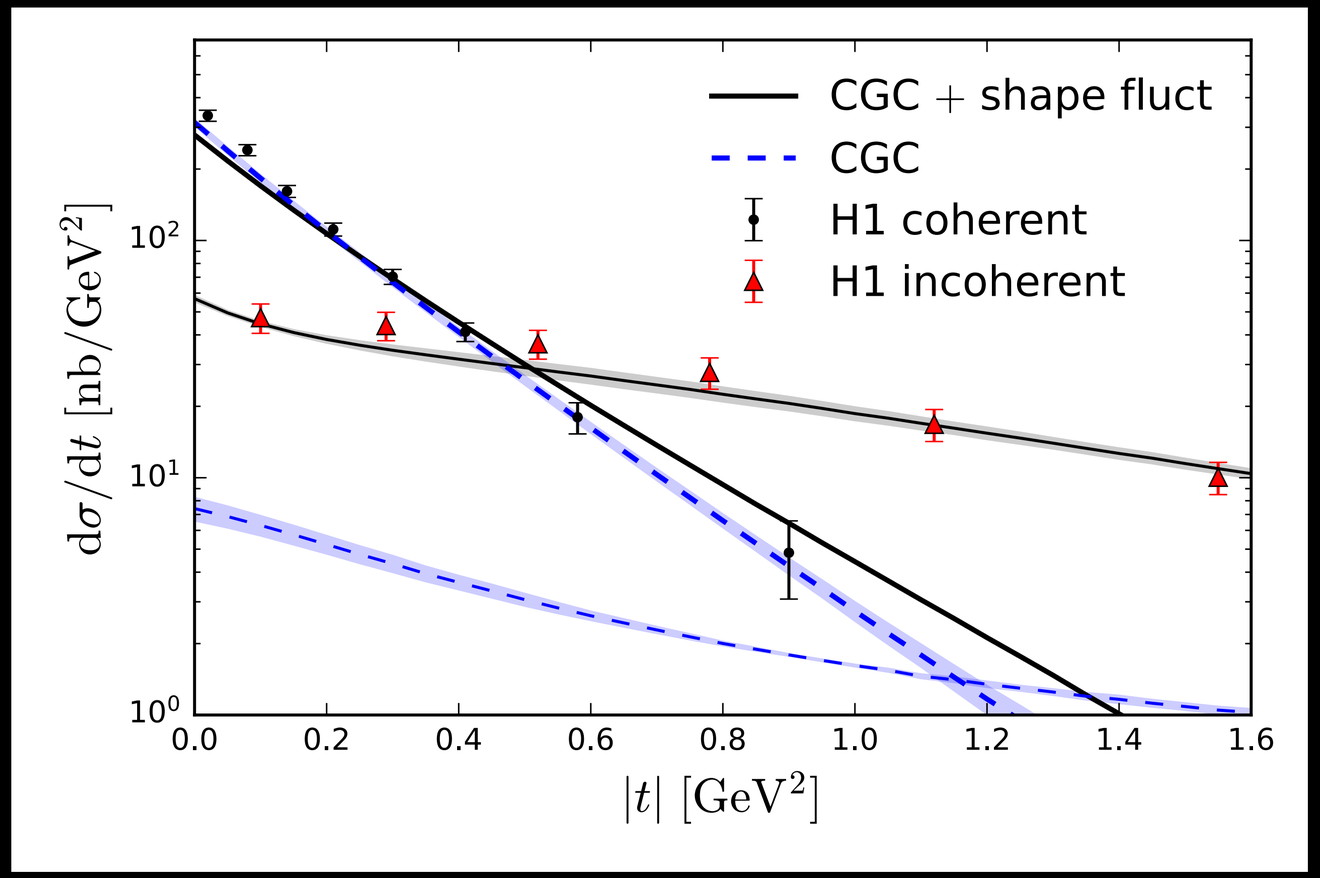

H1 collaboration, Eur. Phys. J. C73 (2013) no. 6 2466

Energy evolution - JIMWLK

H. Mäntysaari, B. Schenke, Phys.Rev.D 98 (2018) 3, 034013; B. Schenke, Rept. Prog. Phys. 84 (2021) 8, 082301

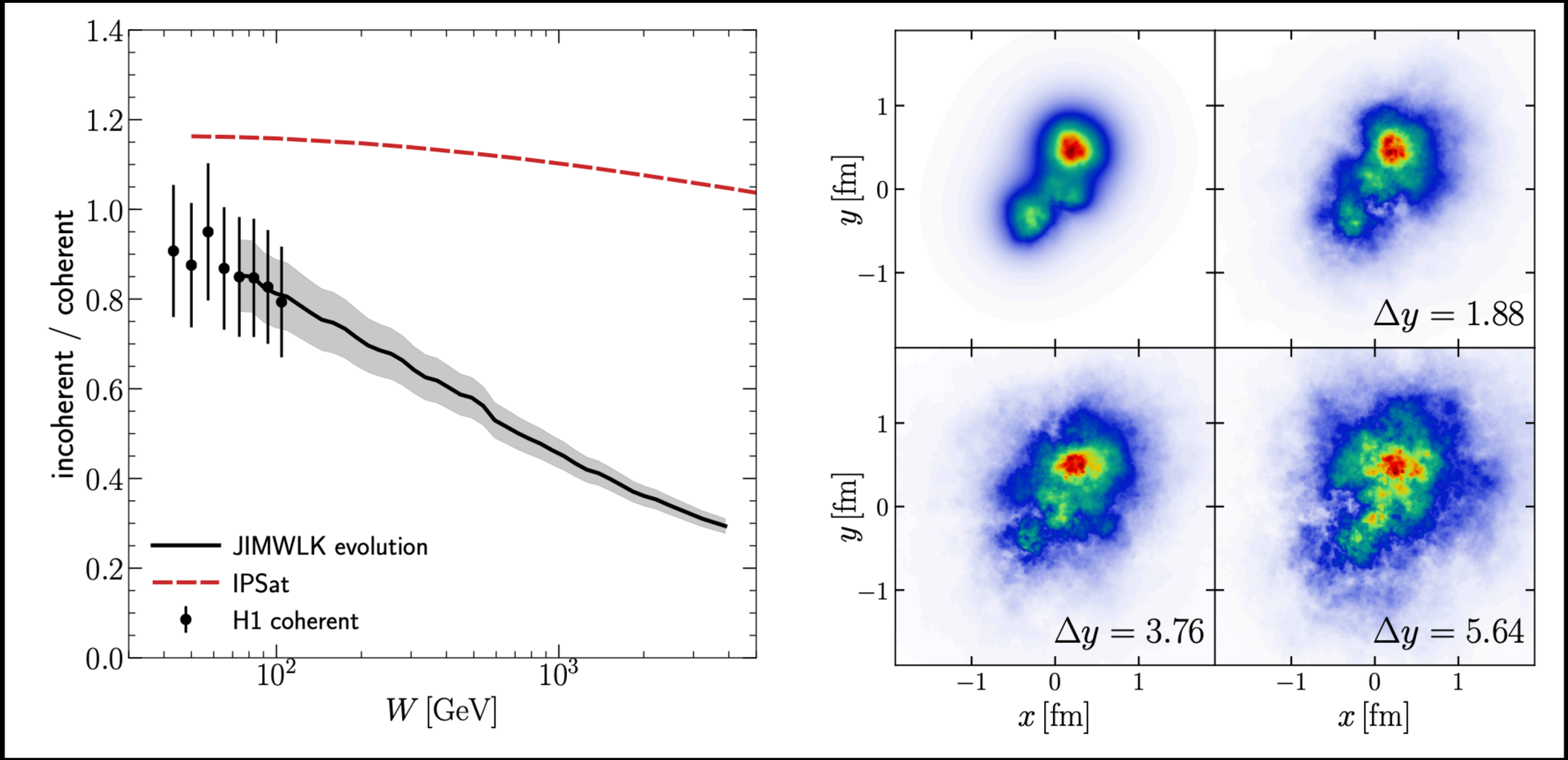

H1 collaboration, Eur. Phys. J. C73 (2013) no. 6 2466

Energy evolution - JIMWLK

H. Mäntysaari, B. Schenke, Phys.Rev.D 98 (2018) 3, 034013

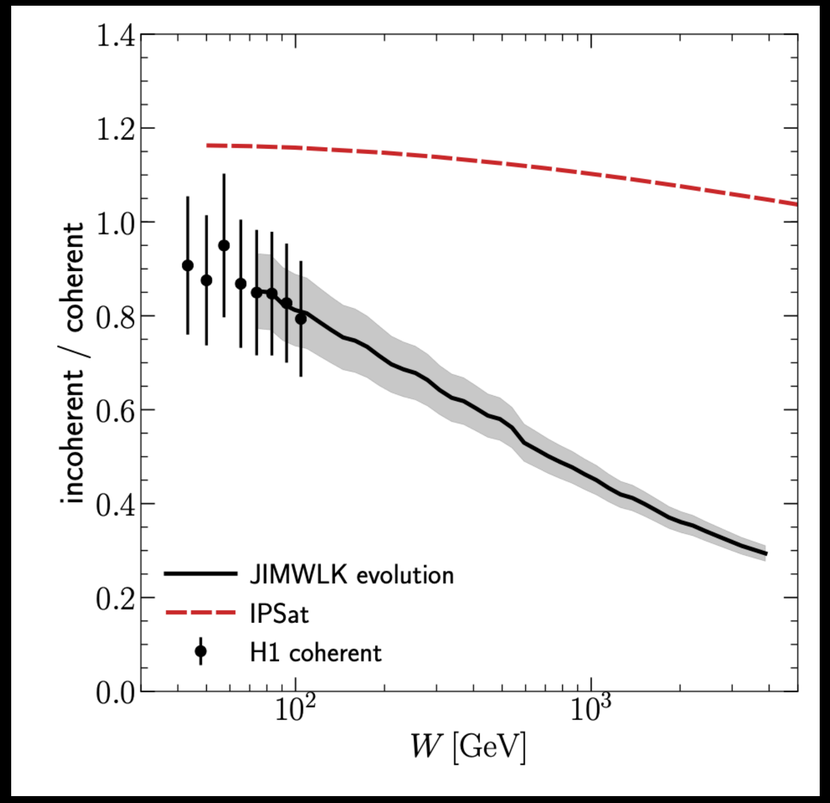

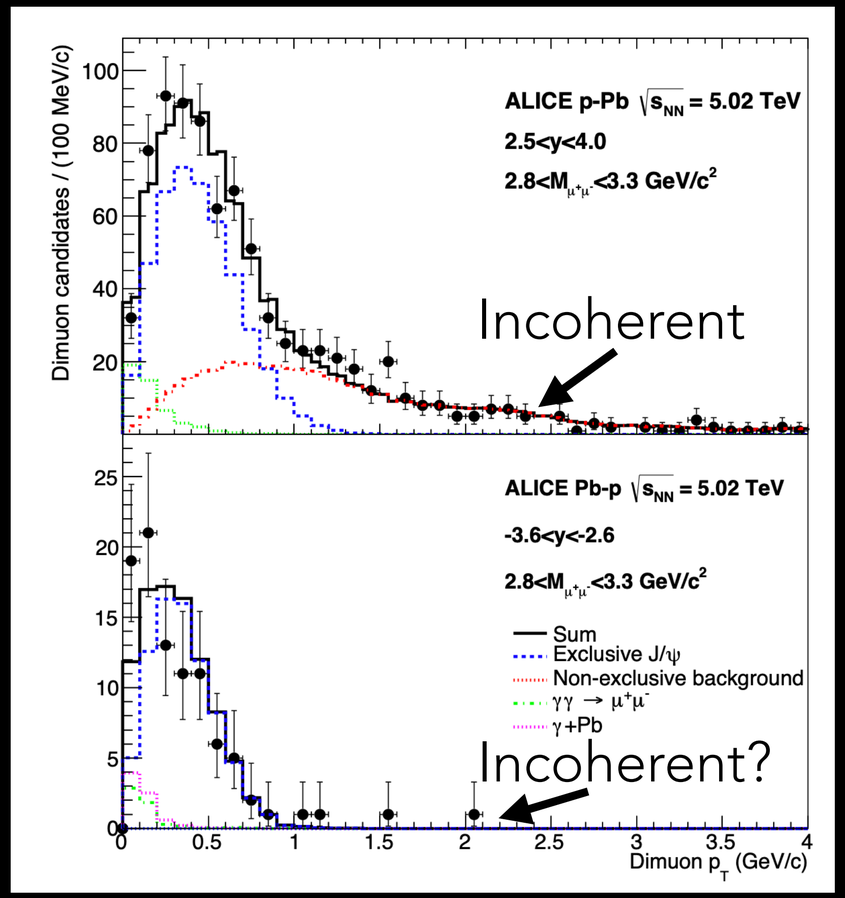

ALICE: arXiv:1406.7819 and 1809.03235

Qualitatively compatible with LHC data:
Small incoherent cross section in high-energy γp scattering

Latest results: Bayesian inference

H. Mäntysaari, B. Schenke, C. Shen, W. Zhao, arXiv:2202.01998 [hep-ph]

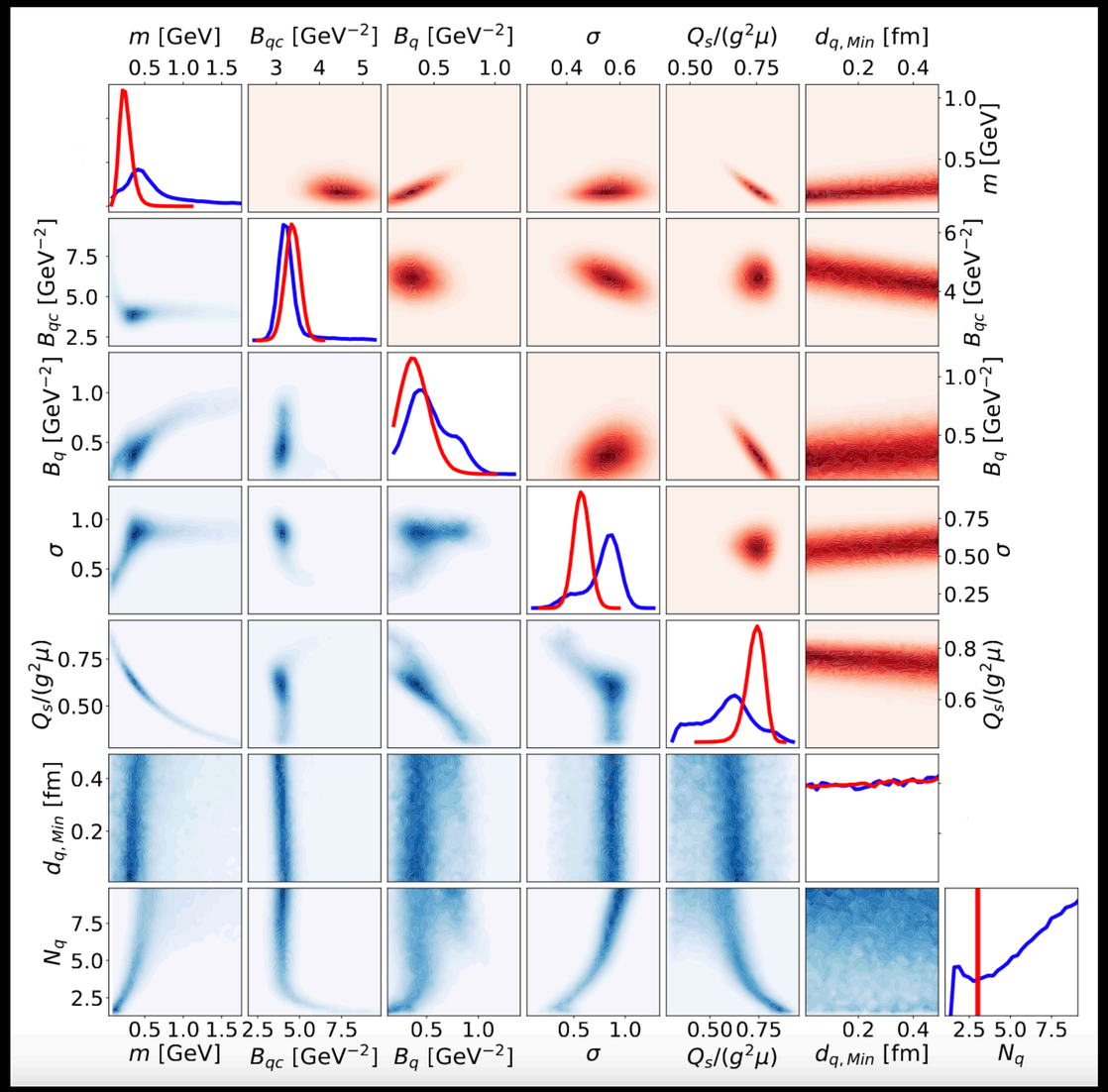

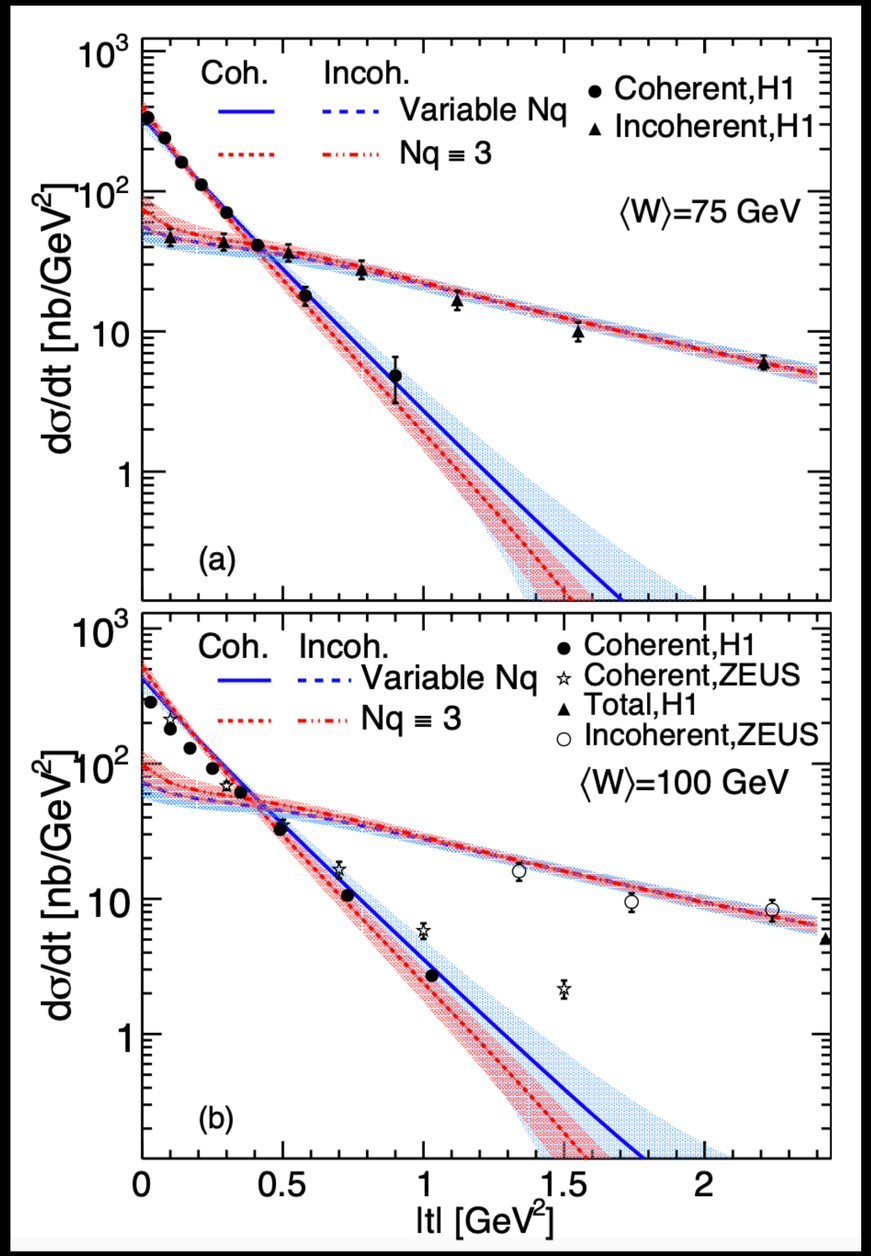

Latest results: Bayesian inference

H. Mäntysaari, B. Schenke, C. Shen, W. Zhao, arXiv:2202.01998 [hep-ph]

See the effect of changing parameters on the cross sections at

https://share.streamlit.io/chunshen1987/ipglasmadiffractionstreamlit/main/IPGlasmaDiffraction_app.py

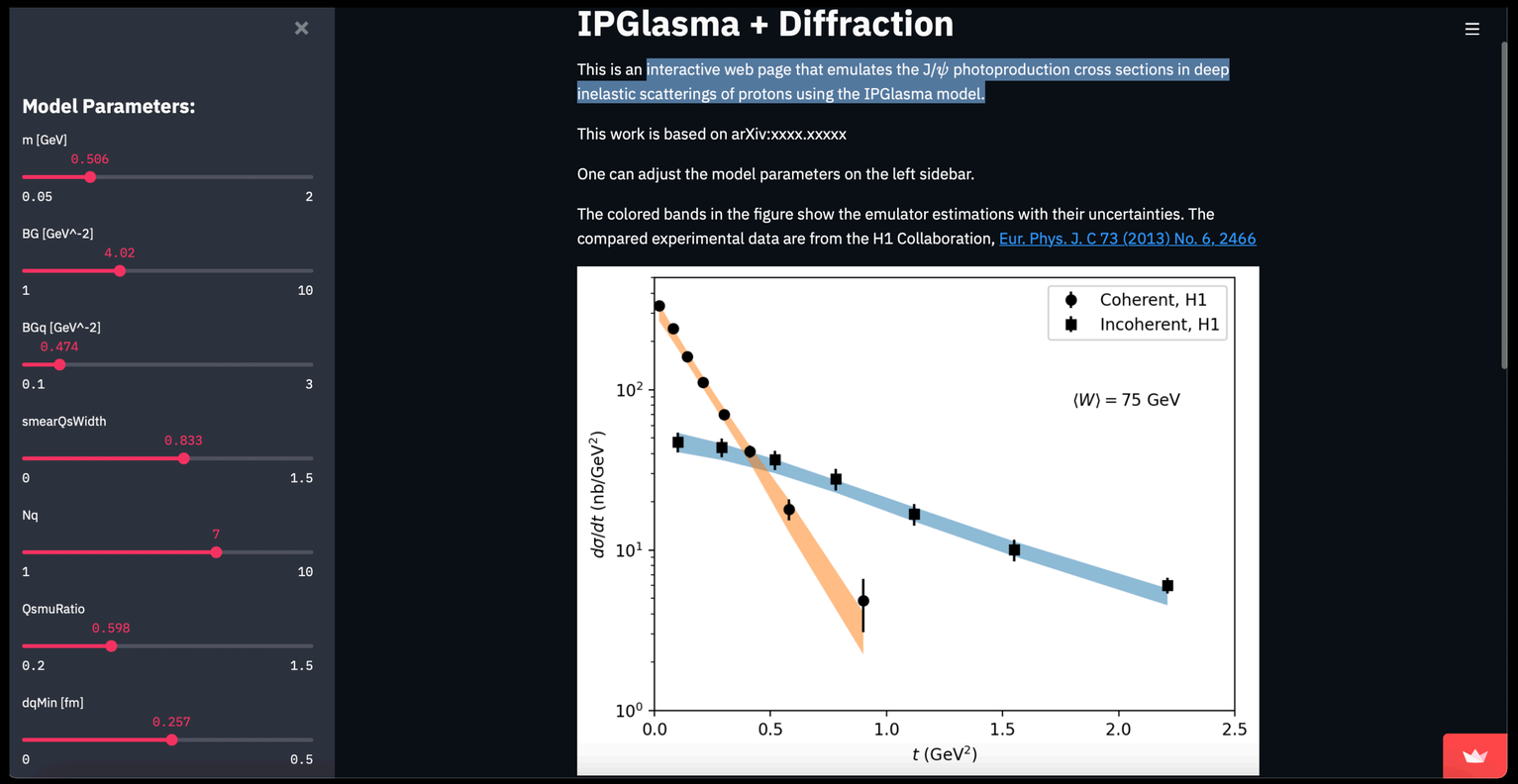

This website also provides posterior samples for your own application

Ultraperipheral collisions (UPC)

- At an impact parameter $|b_T| > 2R_A$ nuclei are photon sources

- Photons are quasi-real $Q^2 \simeq 0$

- High energy $\gamma + \gamma$, $\gamma + p$, $\gamma + A$ at RHIC and LHC

- Focus on $\gamma + p$ and $\gamma + A$ and study diffractive production of vector mesons:

  At small *x* target is mostly gluons

$$\frac{d\sigma^{\gamma^* A \to VA}}{dt} \propto \left[xg(x, Q^2)\right]^2$$ (gluon distribution squared)

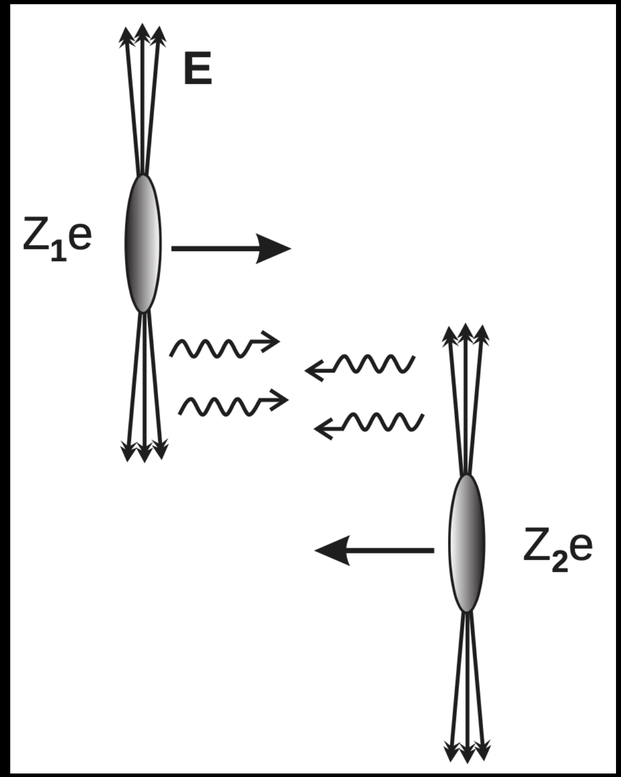

Ultraperipheral collisions (UPC)

C. A. Bertulani, S. R. Klein and J. Nystrand, Ann. Rev. Nucl. Part. Sci. 55 (2005) 271

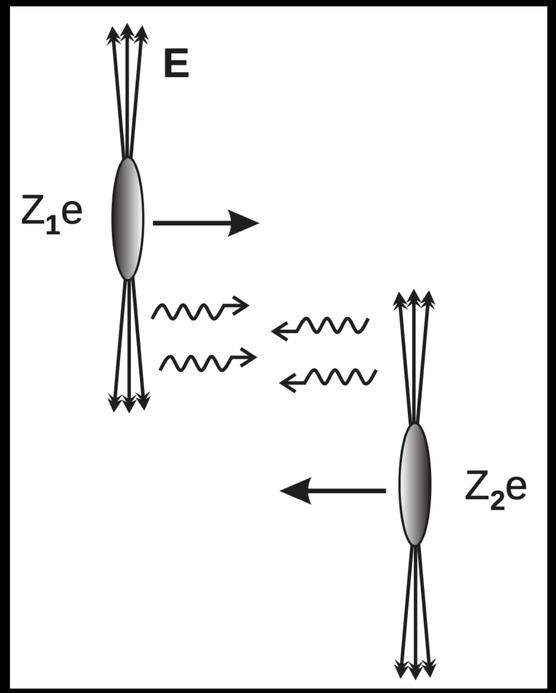

Higher energy in $\gamma + p$ than at HERA

Can study $\gamma A \rightarrow VA$ even before the EIC is built

Ignoring interference, cross section is convolution of photon flux n^{A_1} from nucleus A_1 and γA_2 cross section (and vice versa):

$$\frac{d\sigma^{AA\rightarrow J/\psi AA'}}{dt} = n^{A_2}(\omega_2)\,\sigma^{\gamma A_1}(y) + n^{A_1}(\omega_1)\,\sigma^{\gamma A_2}(-y)$$

y is the rapidity of the J/ψ

$\omega_{1/2}$ are the photon energies

Ultraperipheral collisions (UPC)

C. A. Bertulani, S. R. Klein and J. Nystrand, Ann. Rev. Nucl. Part. Sci. 55 (2005) 271

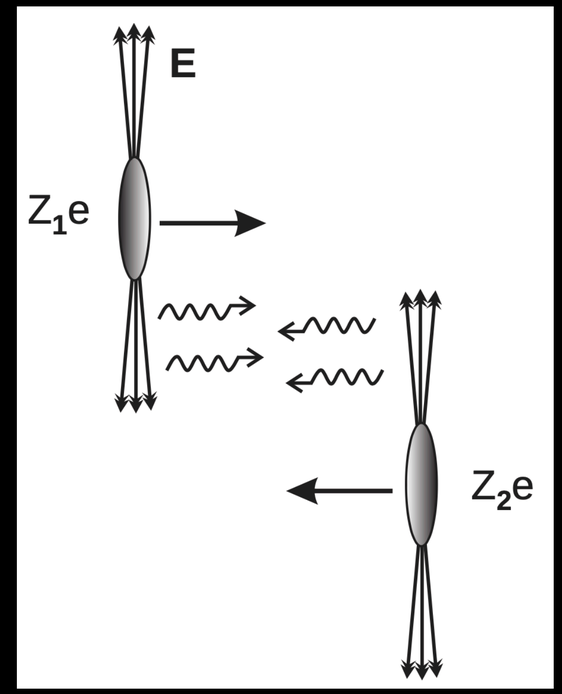

Interference is important in A+A, especially at mid-rapidity. There

$$\frac{d\sigma}{d|t|} = \frac{1}{16\pi}\int d^2\mathbf{B}\,|A_1 - A_2|^2\,\theta(|\mathbf{B}| - 2R_A)$$

Interference is destructive in A+A because of negative parity of the VM

$$\left.\frac{d\sigma^{A_1+A_2\to V+A_1+A_2}}{d|t|dy}\right|_{y=0} = 2\int d^2\mathbf{B}\,n(\omega,|\mathbf{B}|)\frac{d\sigma^{\gamma+A\to V+A}}{d|t|}[1-\cos(\boldsymbol{\Delta}\cdot\mathbf{B})]\,\theta(|\mathbf{B}| - 2R_A)$$

J/ψ in Pb+Pb UPCs: Subnucleonic fluctuations

H. Mäntysaari, B. Schenke, Phys.Lett.B 772 (2017) 832-838, arXiv:1703.09256

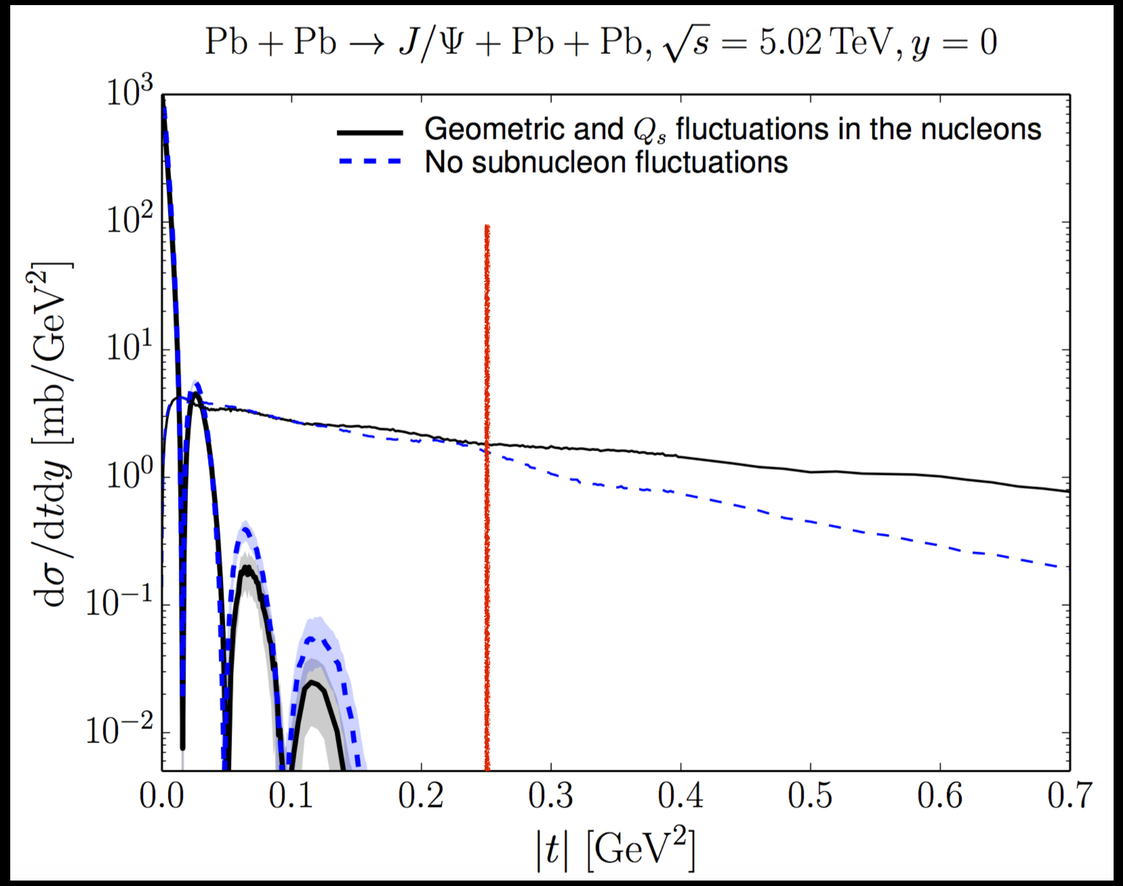

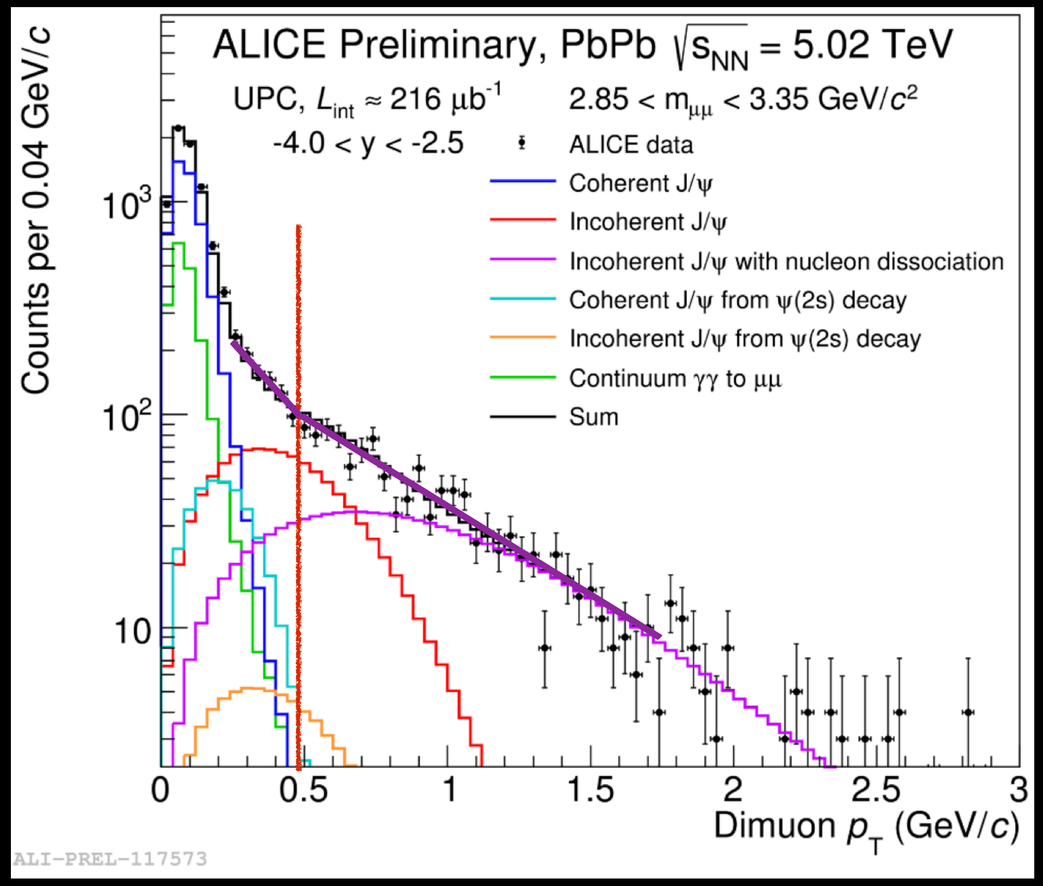

Coherent: thick lines

Incoherent: thin lines

Fix normalization in e+p

H. Mäntysaari, F. Salazar, B. Schenke, in preparation

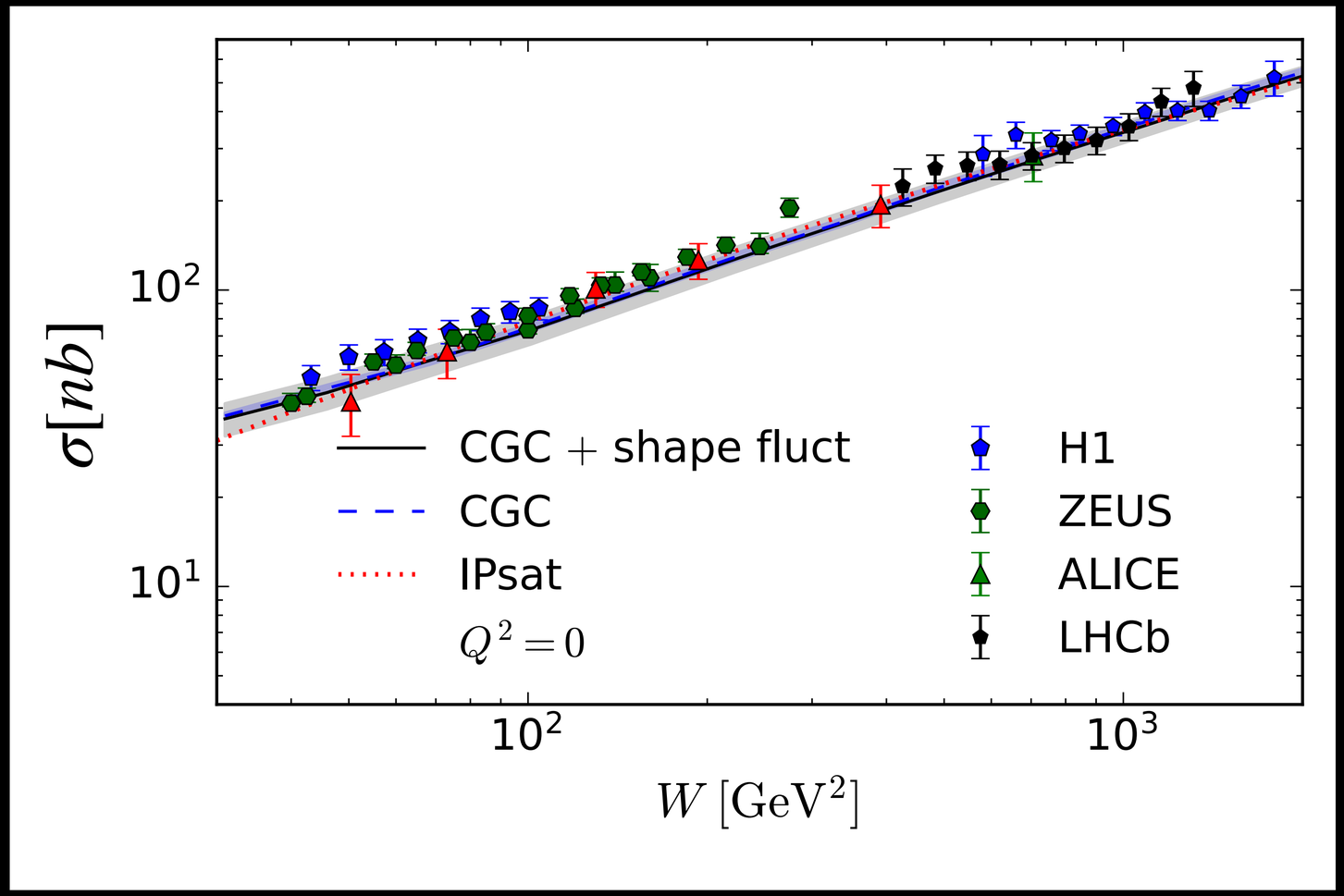

Make sure we get the normalization right in both cases: with and w/o shape fluctuations

First compare to ALICE γ+Pb measurement

H. Mäntysaari, F. Salazar, B. Schenke, in preparation

Here, ALICE removed interference and photon k_T effects to get the γ+Pb cross section

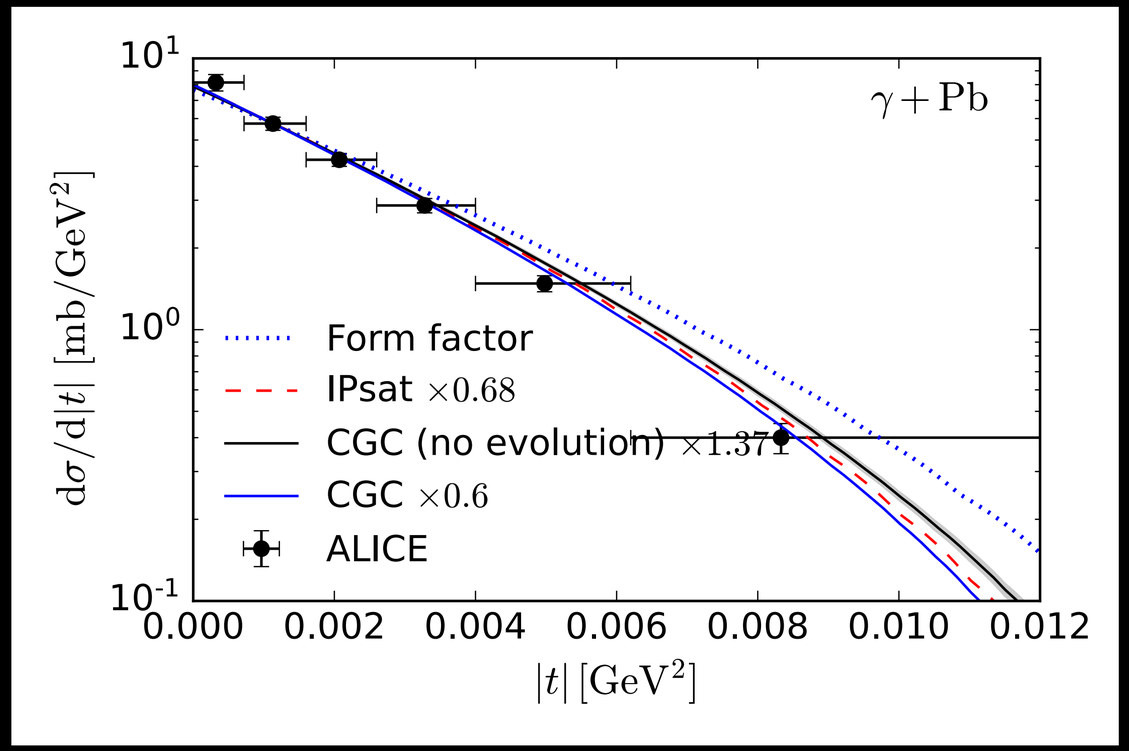

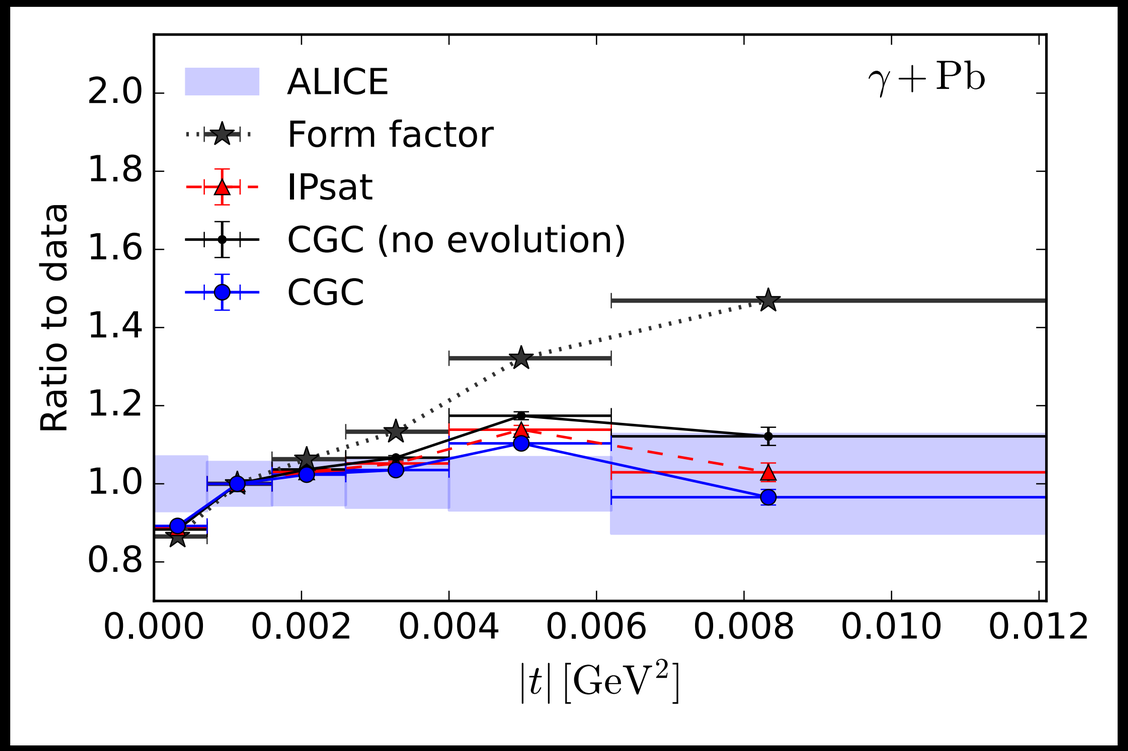

Saturation effects improve agreement with experimental data significantly

|t| integrated coherent cross section

H. Mäntysaari, F. Salazar, B. Schenke, in preparation

Pb+Pb → Pb+Pb+J/ψ

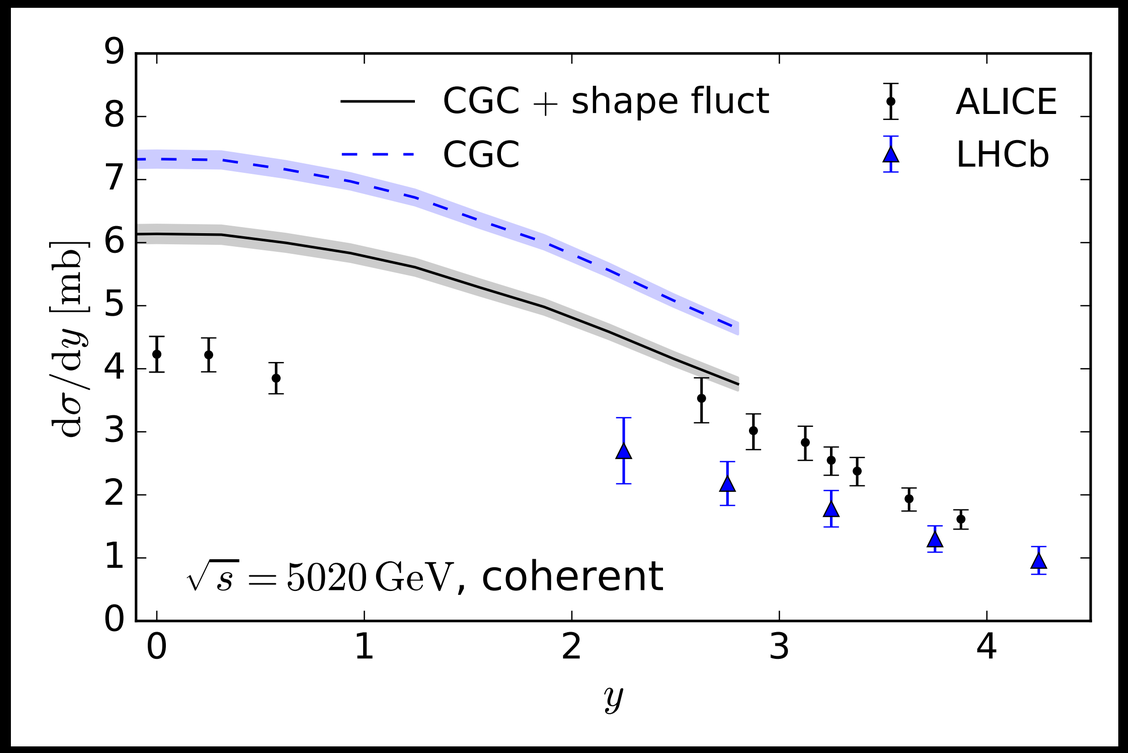

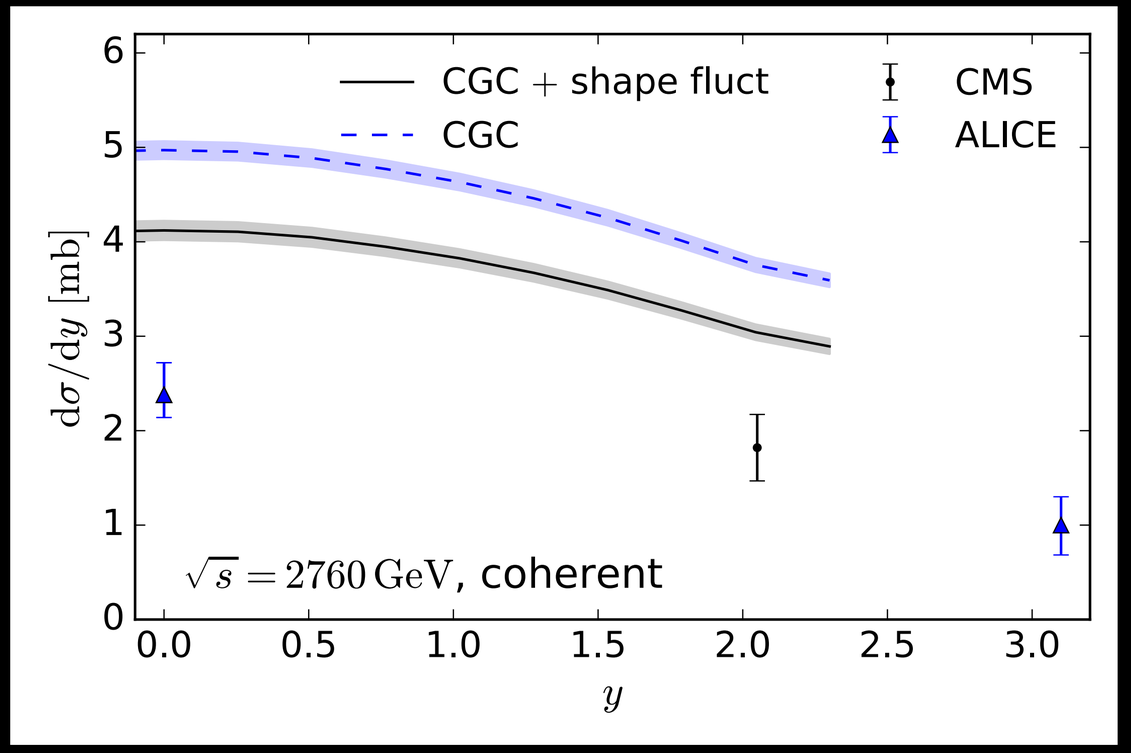

Larger suppression when including shape fluctuations: Hotter hot spots; larger local Q_s

ALICE arXiv:2101.04577; Phys. Lett. B798 (2019) 134926; Phys. Lett. B718 (2013) 1273;
Eur. Phys. J. C73 (2013) no. 11 2617; LHCb arXiv:2107.03223; CMS Phys. Lett. B772 (2017) 489

|t| integrated incoherent cross section

H. Mäntysaari, F. Salazar, B. Schenke, in preparation

Pb+Pb → Pb+Pb+J/ψ

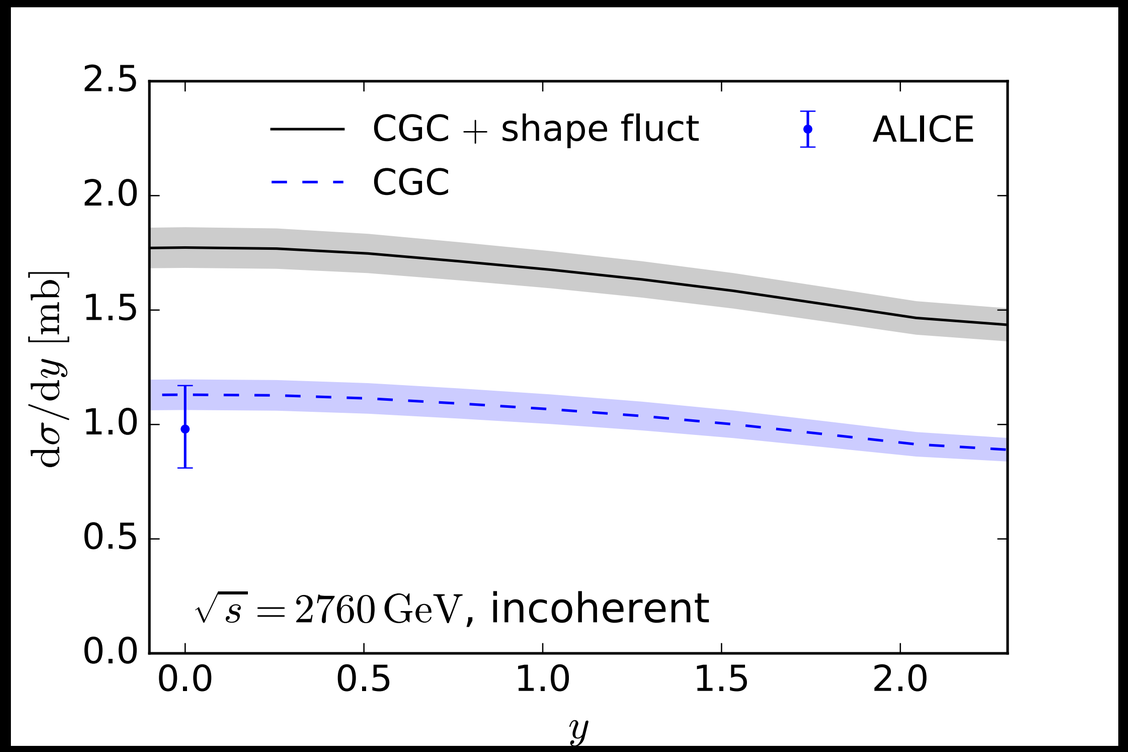

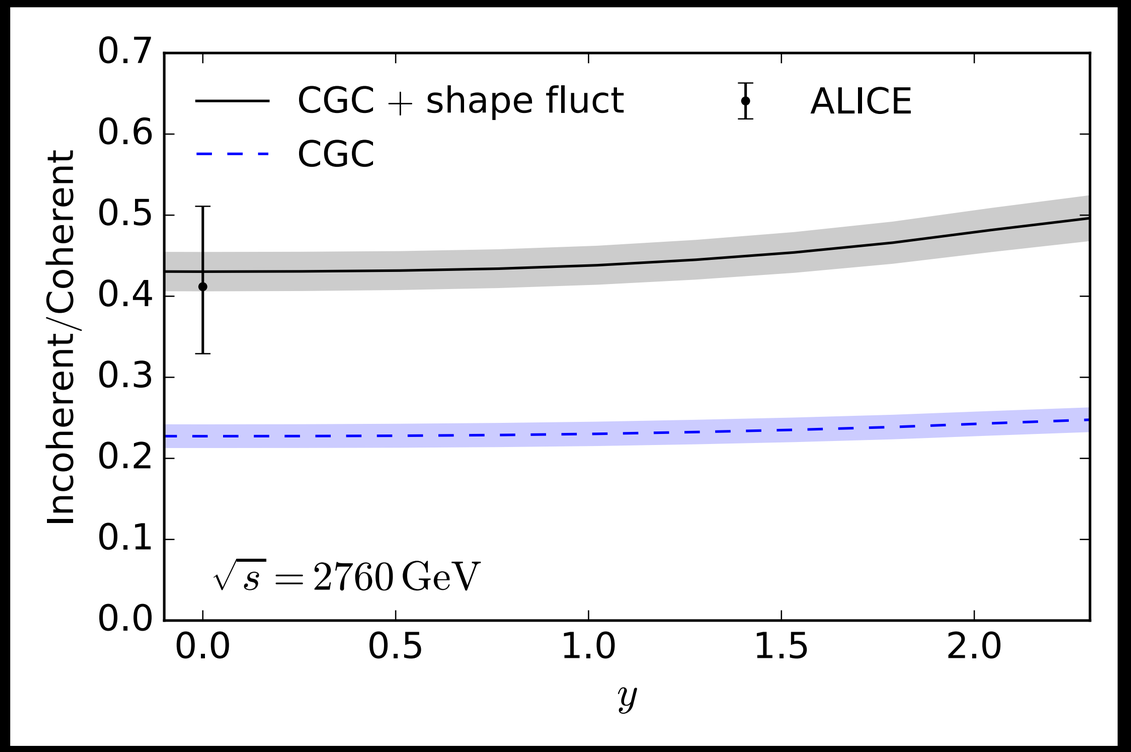

More fluctuations when including shape fluctuations → larger incoherent cross section

Ratio of coherent to incoherent well described (both coh. and incoh. overestimated)

ALICE Eur. Phys. J. C73 (2013) no. 11 2617

Photoproduction of J/ψ in d+Au collisions at STAR

H. Mäntysaari, B. Schenke, Phys. Rev. C101, 015203 (2020)

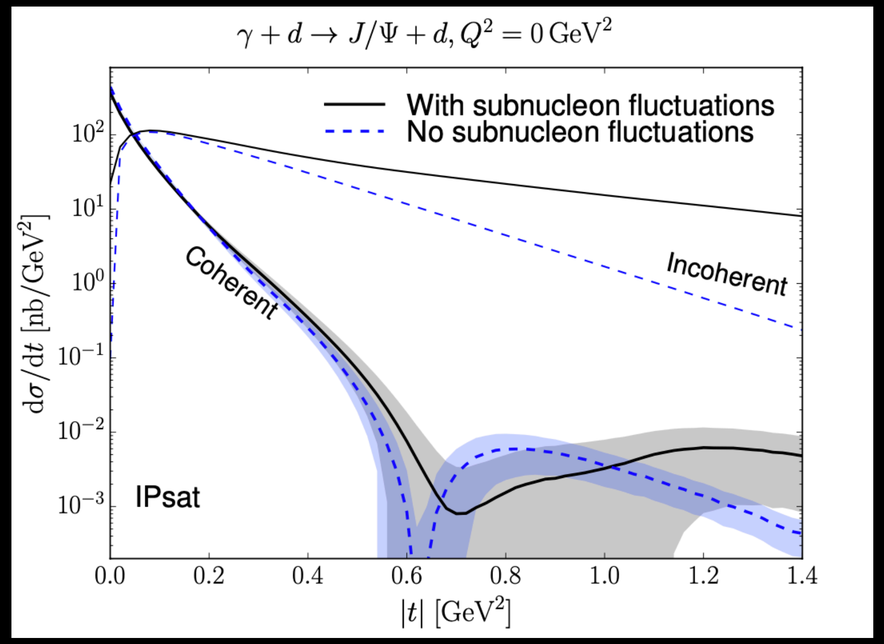

Can also access details of deuteron wave function

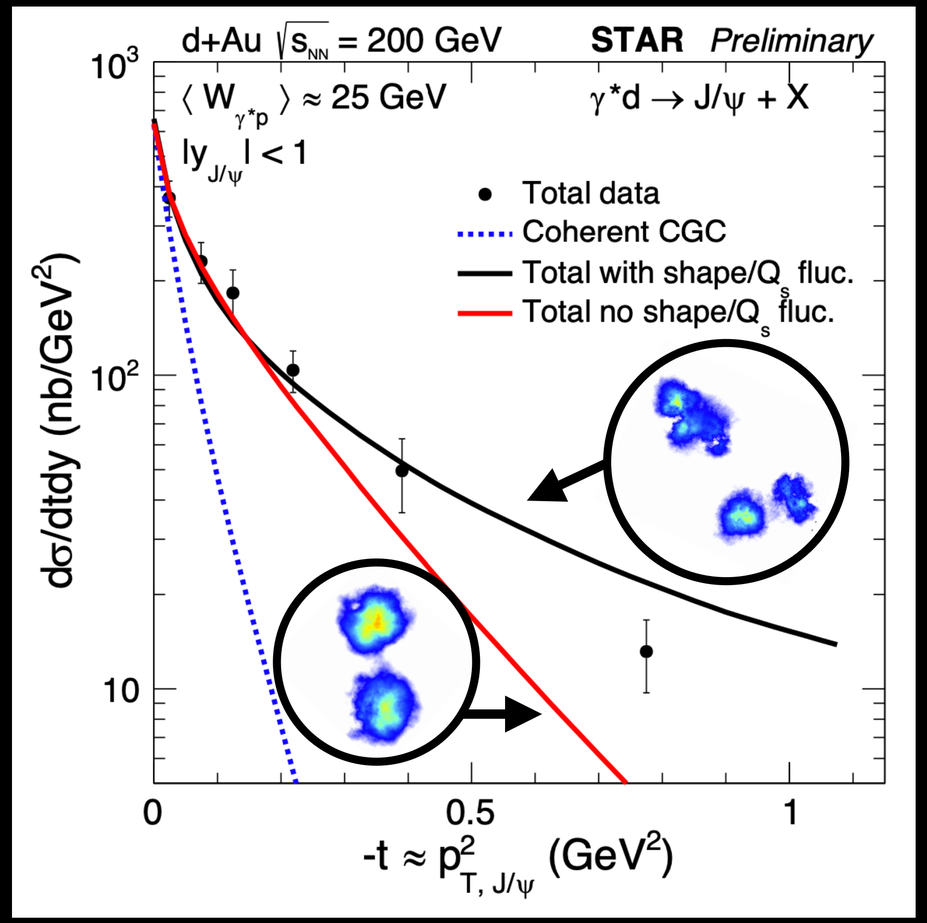

STAR Collaboration at Hard Probes 2020

PoS HardProbes2020 (2021) 100; arXiv:2009.04860

Substructure: large effect on incoherent at $|t| \gtrsim 0.25\mathrm{GeV}^2$ (as in Pb)

STAR data favors substructure

Photoproduction of J/ψ in d+Au collisions at STAR

H. Mäntysaari, B. Schenke, Phys. Rev. C101, 015203 (2020)

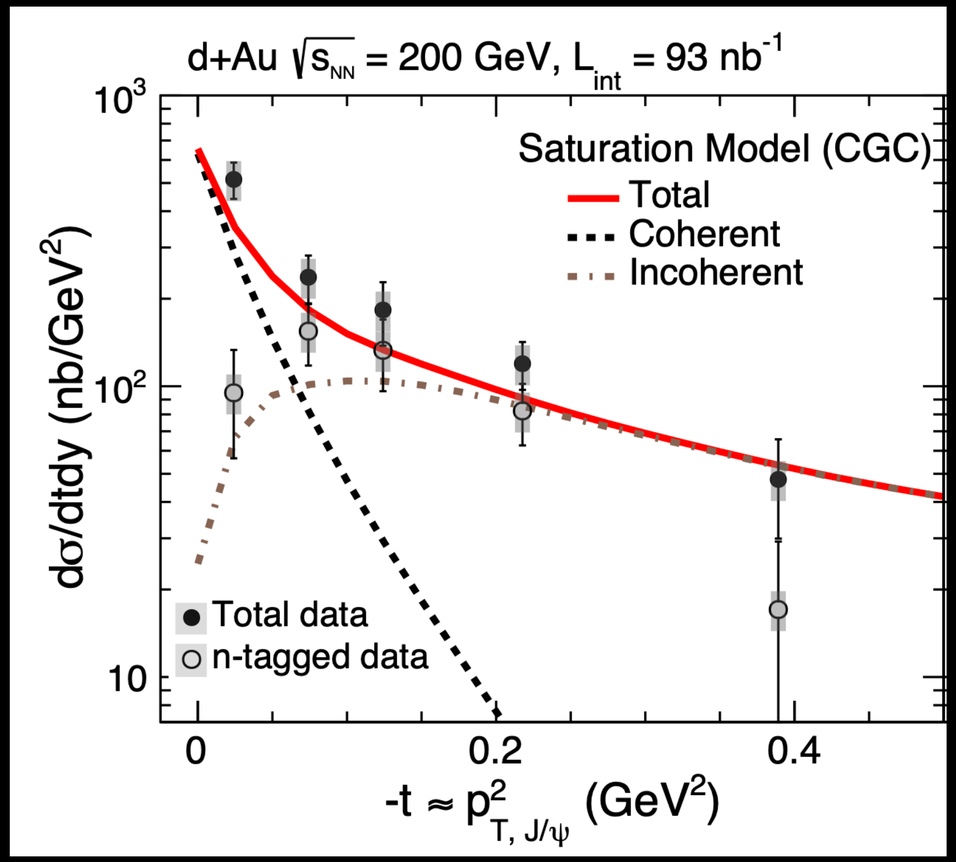

n-tagged results can be compared to incoherent cross section

STAR Collaboration, e-Print: 2109.07625

Saturation effects: Dependence on Q^2 and A

H. Mäntysaari, R. Venugopalan, Phys. Lett. B781 (2018) 664-671

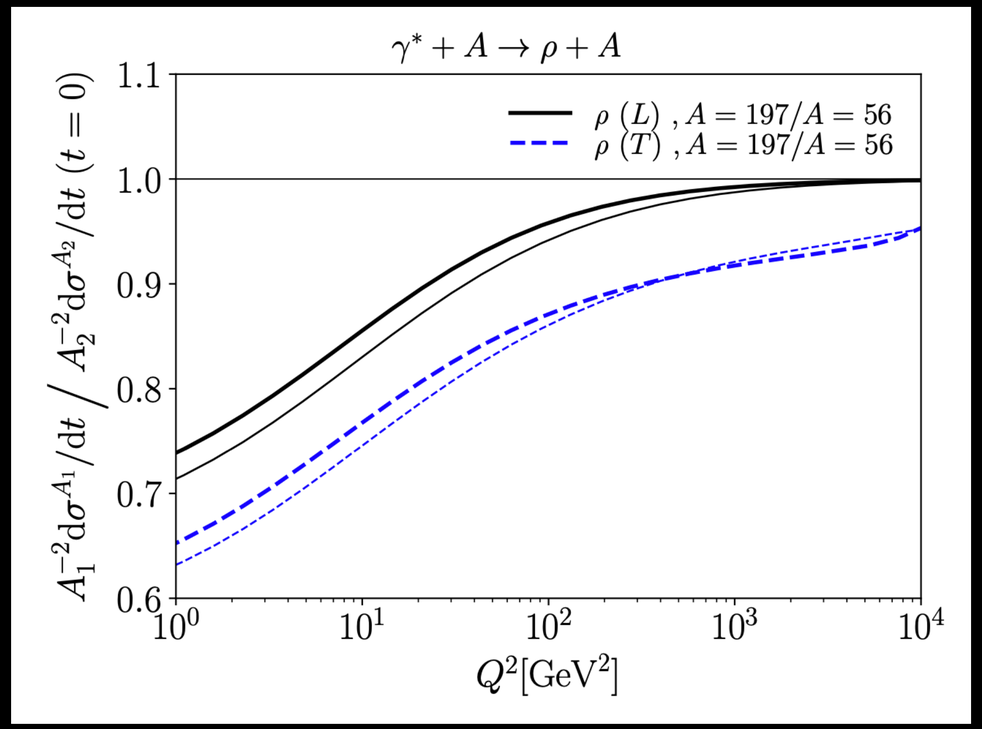

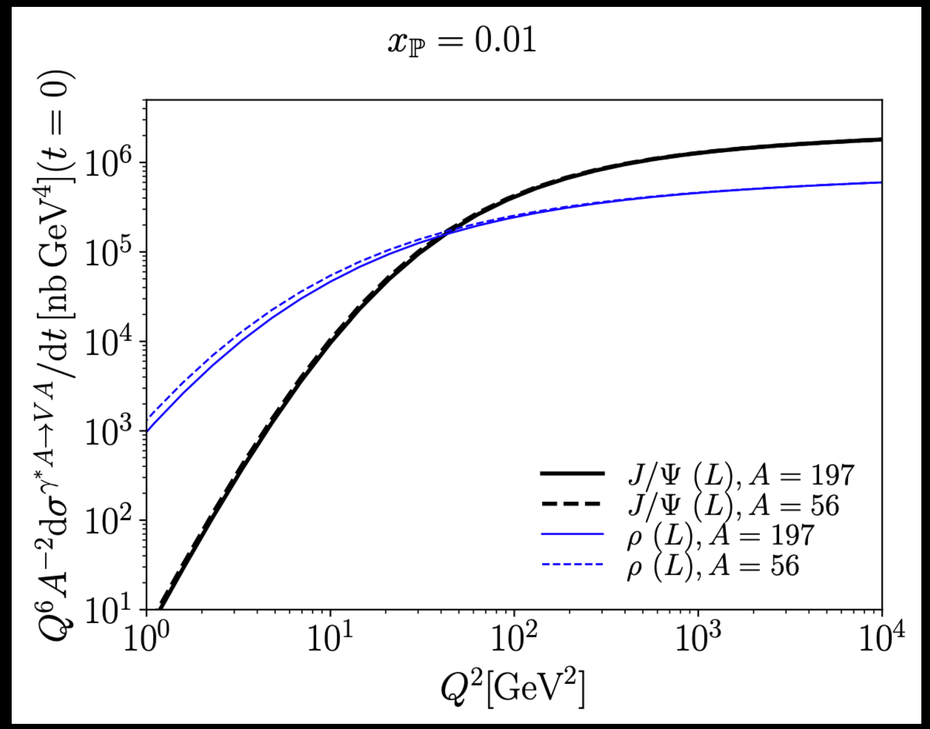

- At large Q^2 expect scaling $\propto A^2$ for $|t| = 0$; Saturation effects for smaller Q^2
- Longitudinal x-sec scales as Q^{-6} for large Q^2, and as Q^2 for small $Q^2 \ll Q_s^2$

Summary and Outlook

- Coherent and incoherent diffraction at small *x* provide information on spatial gluon distribution and its fluctuations + saturation
- Constrained parameters using Bayesian analysis
- Nucleon substructure has a significant effect on the incoherent cross section at $|t| \gtrsim 0.25\,\mathrm{GeV}^2$
- Saturation affects shape of $|t|$ spectra and scaling with A and Q^2
- γ + d collisions at RHIC: Substructure fluctuations improve description of experimentally observed $|t|$ dependence!
- Next: Go to NLO. A lot of progress: e.g. **H. Mäntysaari, J. Penttala, arXiv:2104.02349**

BACKUP

Light nuclei: Nucleon distributions

H. Mäntysaari, B. Schenke, Phys. Rev. C101, 015203 (2020)

Nucleon distributions:

- Deuteron wave function:
  - Argonne v18 (AV18)
  - Hulthen:

R. B. Wiringa, V. G. J. Stoks and R. Schiavilla, Phys. Rev. C51 (1995) 38
www.phy.anl.gov/theory/research/density2

$$\phi_{\rm pn}(d_{\rm pn}) = \frac{1}{\sqrt{2\pi}} \frac{\sqrt{ab(a+b)}}{b-a} \frac{e^{-ad_{\rm pn}} - e^{-bd_{\rm pn}}}{d_{\rm pn}}$$

$$a = 0.228\,\mathrm{fm}^{-1}$$
$$b = 1.18\,\mathrm{fm}^{-1}$$

see M. L. Miller, K. Reygers, S. J. Sanders, P. Steinberg, Ann. Rev. Nucl. Part. Sci. 57 (2007) 205

- ^{3}He wave function:
  - AV18+UIX J. Carlson and R. Schiavilla, Rev. Mod. Phys. 70 (1998) 743

    same configurations as available in PHOBOS MC-Glauber

    C. Loizides, J. Nagle and P. Steinberg, arXiv:1408.2549

Light nuclei: Nucleon distributions

H. Mäntysaari, B. Schenke, Phys. Rev. C101, 015203 (2020)

Deuteron size distributions

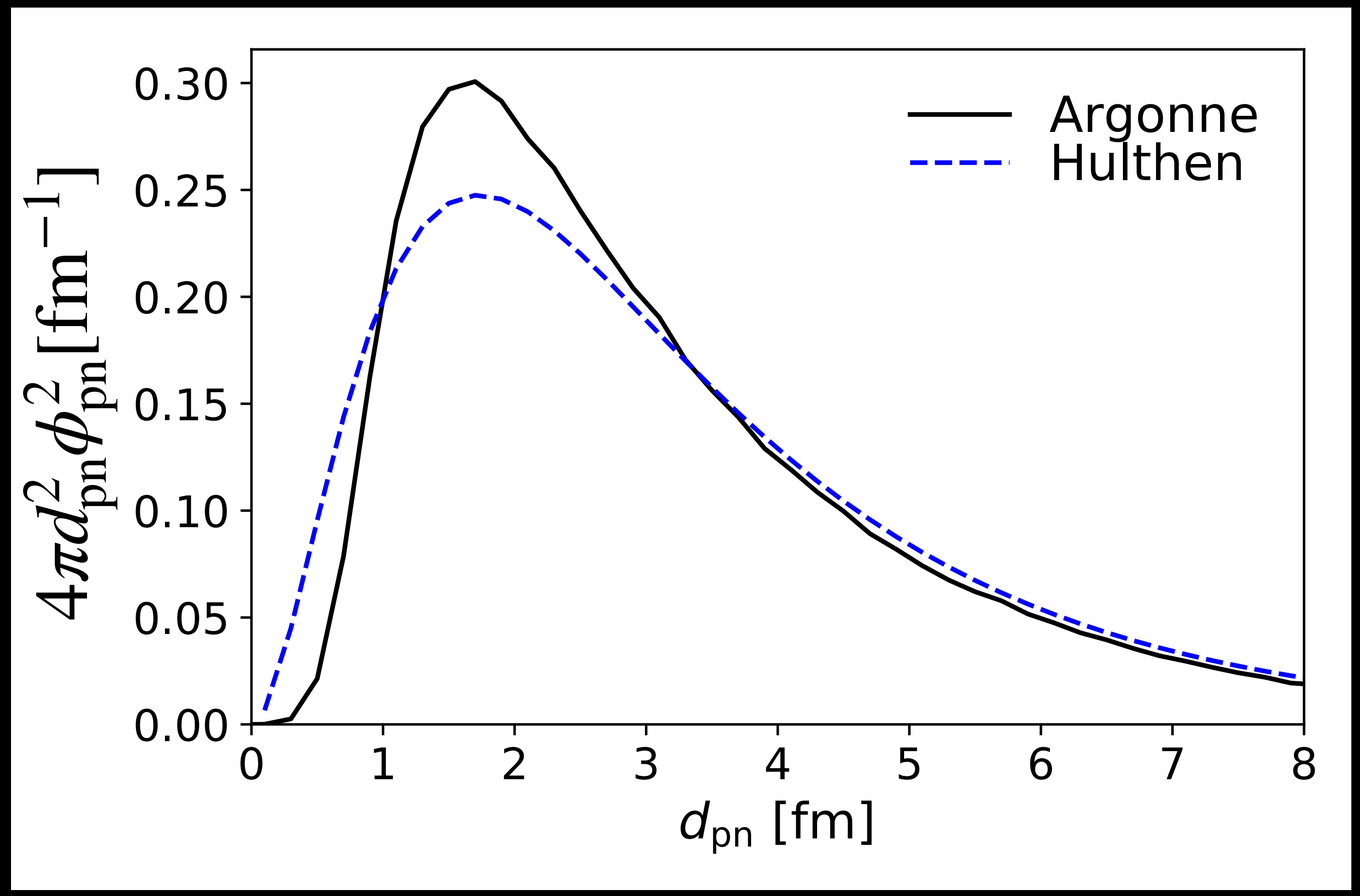

We need the gluon distribution

Assumption:

Small *x* gluon structure follows the large *x* nucleon structure

Predictions for the EIC: Effect of deuteron wave function

H. Mäntysaari, B. Schenke, Phys. Rev. C101, 015203 (2020)

J/Ψ production for $\sqrt{s} = 140\sqrt{Z/A}\,\mathrm{GeV}$

such that x_P can reach down to 10^{-4} to 10^{-3}

$$x_P = \frac{Q^2 + M_V^2 - t}{Q^2 + W^2 - m_N^2}$$

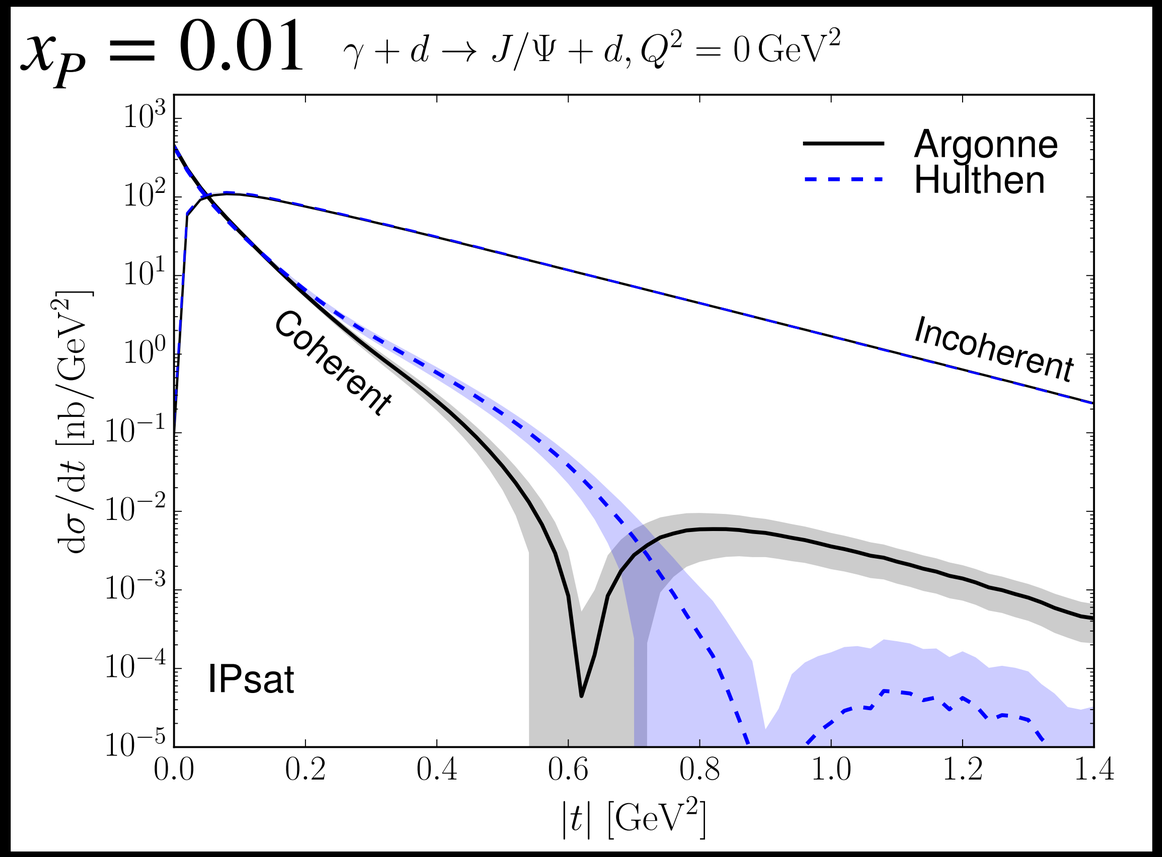

Differences appear at $|t| \gtrsim 0.3\,\mathrm{GeV}^2$
(Long distance behavior is similar)

The two wave functions result in similar rms sizes of the deuteron

Difference in dip position must come from the different average impact parameter profile.

Energy evolution (deuterons)

H. Mäntysaari, B. Schenke, Phys. Rev. C101, 015203 (2020)

IPSat - only normalization changes

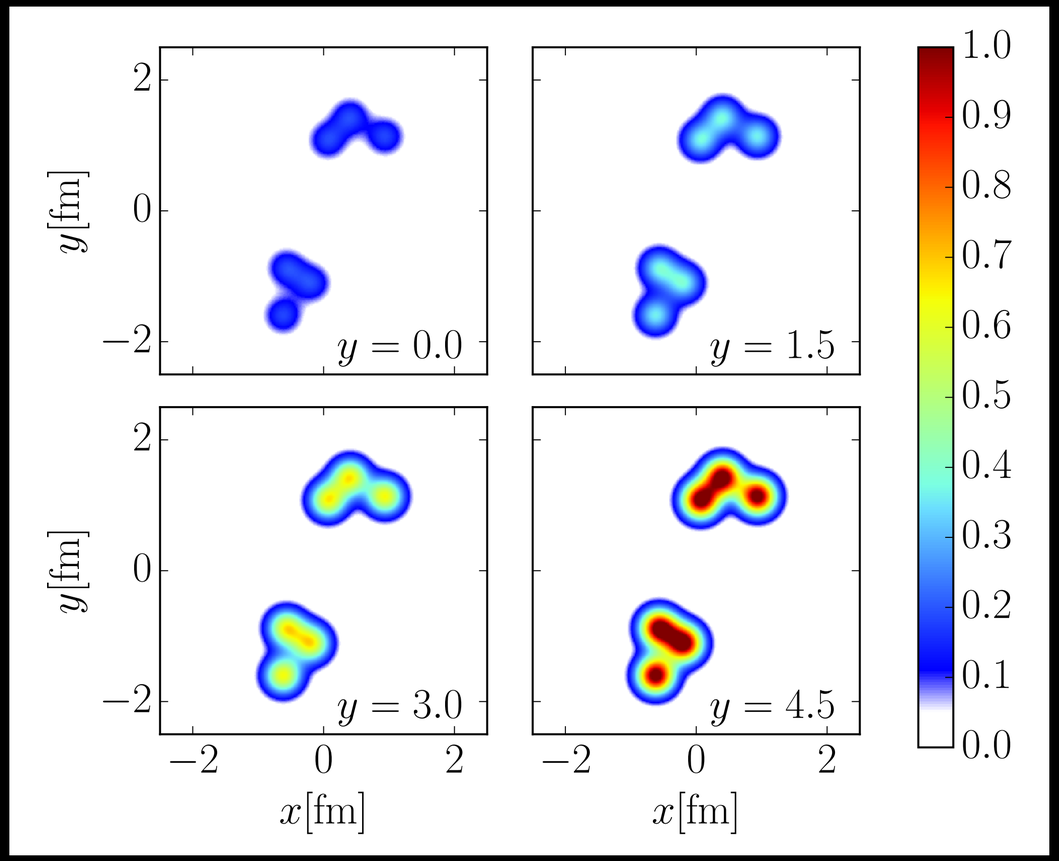

CGC - nucleus grows as well

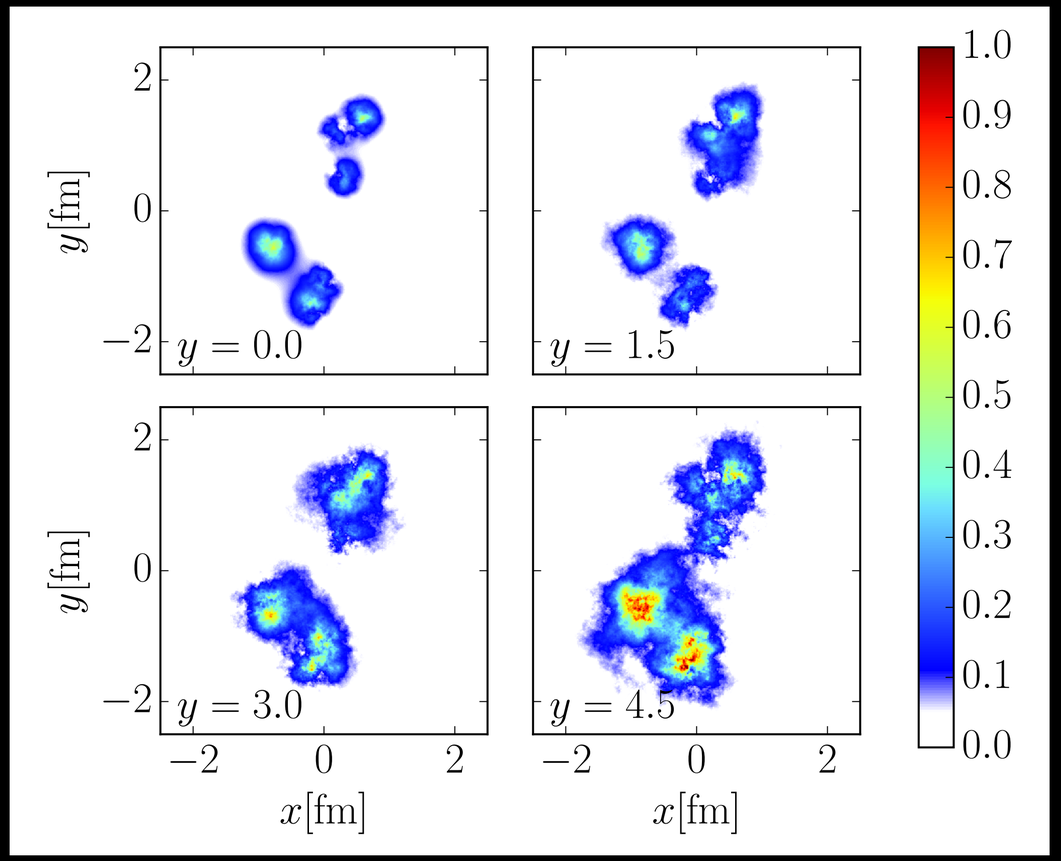

We plot $1 - \mathrm{Re}[\mathrm{tr}(V(\vec{x})]/N_c$

Predictions for the EIC: Small-x evolution

H. Mäntysaari, B. Schenke, Phys. Rev. C101, 015203 (2020)

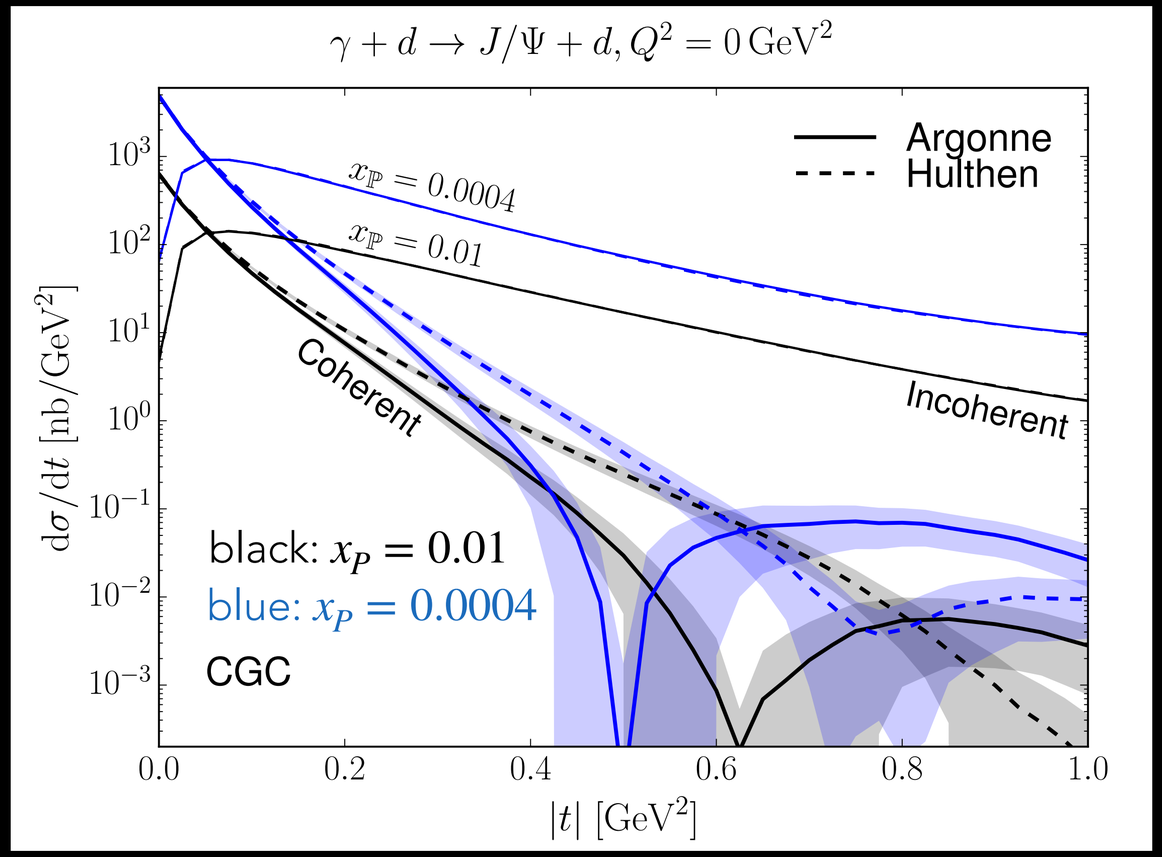

(no nucleon shape fluctuations)

Differences between wave functions survive the JIMWLK evolution

They are not washed out at small x

Dip moves to smaller $|t|$ indicating growth of the average target size

Predictions for the EIC: Target size vs. *x*

H. Mäntysaari, B. Schenke, Phys. Rev. C101, 015203 (2020)

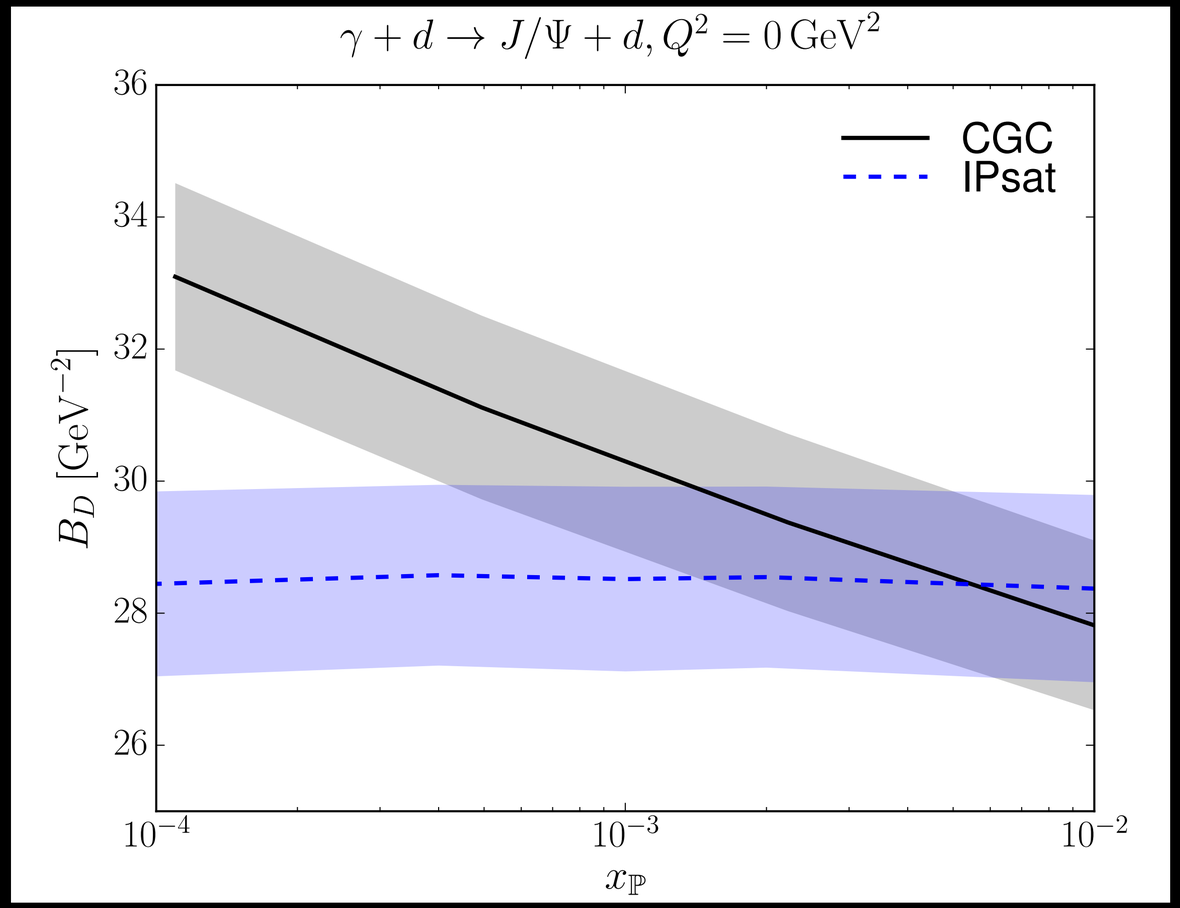

Growth of the target with decreasing *x* is illustrated by extracting B_D from a fit to the coherent cross section at small t using $d\sigma/dt \sim \exp(-B_D|t|)$

IPSat model does not include the growth of the target

Dipole amplitude in e+A scattering

H. Mäntysaari, B. Schenke, Phys. Rev. C101, 015203 (2020)

$$N^{\mathrm{A}}(\vec{r}, \overrightarrow{b}, x) = 1 - \prod_{i=1}^{A} \left[1 - N^{\mathrm{p}}(\vec{r}, \overrightarrow{b} - \overrightarrow{b}_i, x)\right]$$

This is equivalent to summing up the density profiles of the nucleons

We also fluctuate the normalization of Q_s^2 in each hot spot according to

$$P(\ln(Q_s^2/\langle Q_s^2\rangle) = \frac{1}{\sqrt{2\pi}\sigma} \exp\left[- \frac{\ln^2(Q_s^2/\langle Q_s^2\rangle)}{2\sigma^2}\right]$$

with $\sigma = 0.65$ for IPSat

Saturation effects

H. Mäntysaari, B. Schenke, Phys. Rev. C101, 015203 (2020)

Comparing evolution of a deuteron (solid) to two individual nucleons (dotted)

The effect is only visible after substantial evolution

$d_{\mathrm{pn}} = 1.5\,\mathrm{fm}$

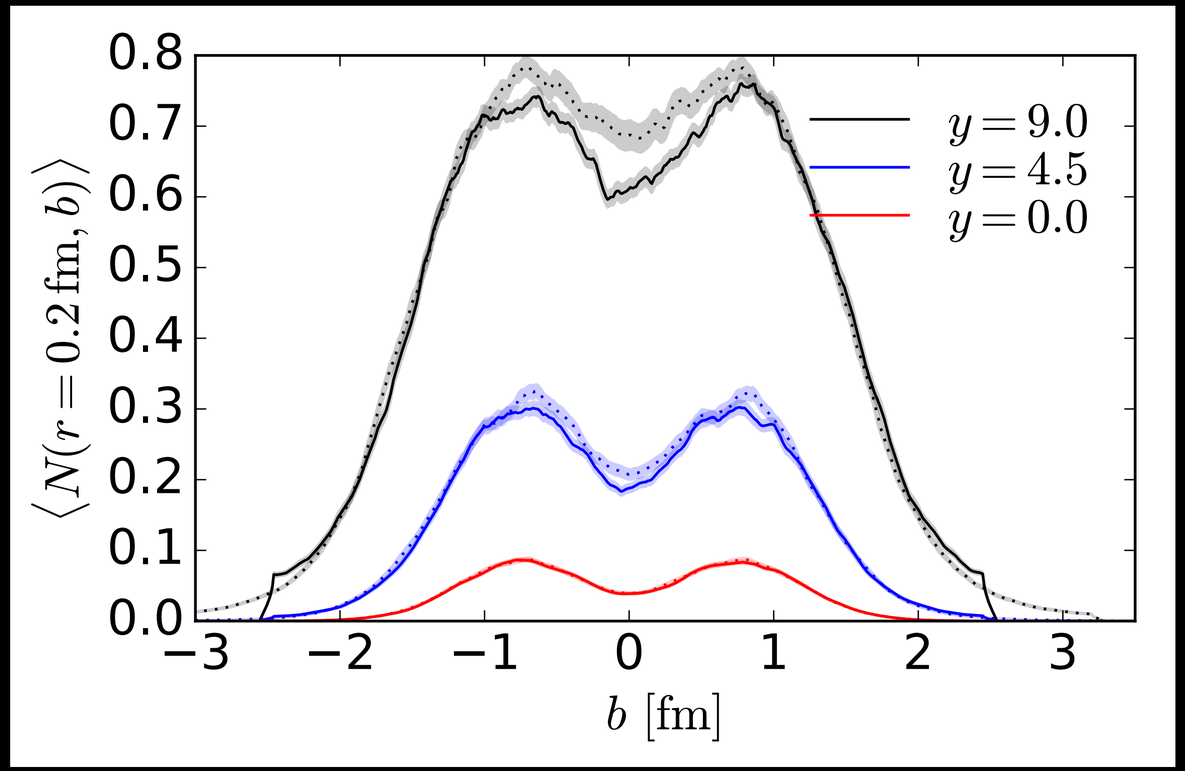

Predictions for the EIC: Effect of nucleon shape fluctuations

H. Mäntysaari, B. Schenke, Phys. Rev. C101, 015203 (2020)

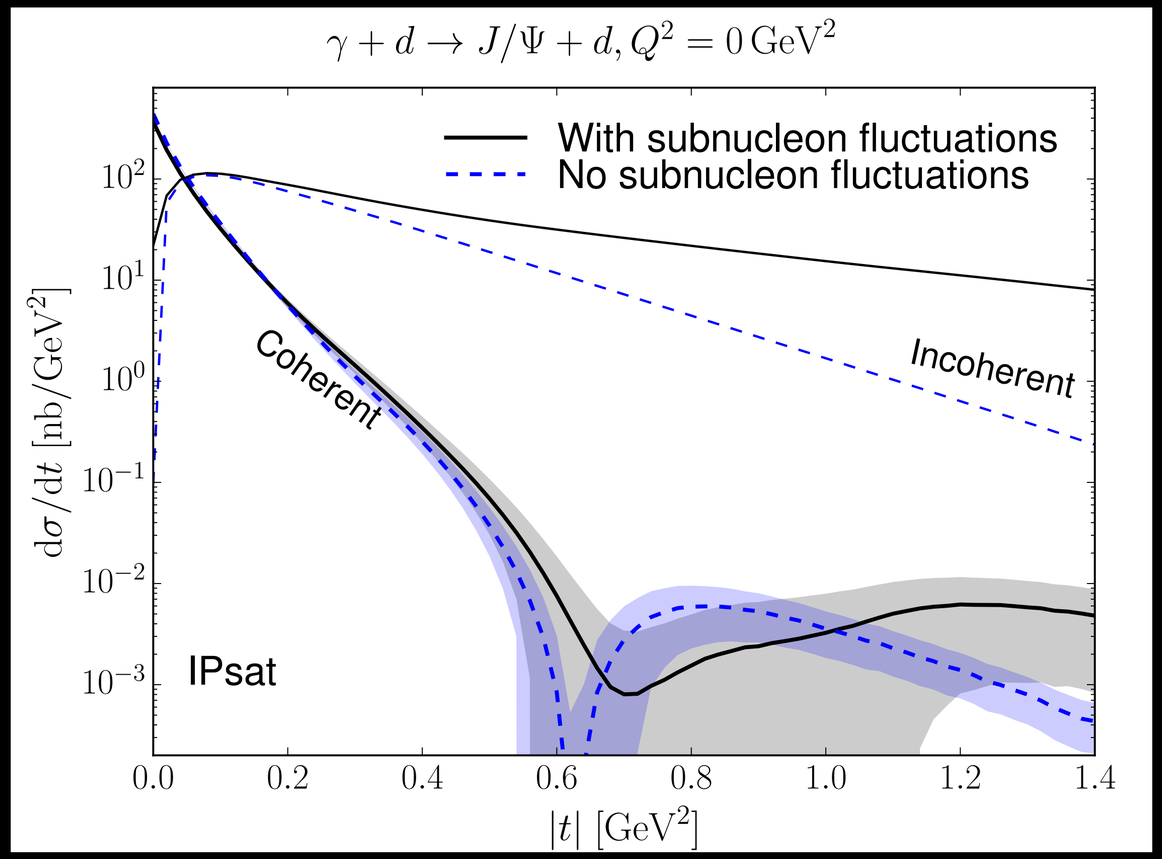

Coherent cross section unchanged (within errors) - average shape is (approximately) the same by construction

Subnucleon fluctuations increase incoherent cross section significantly for $|t| \gtrsim 0.25\,\mathrm{GeV}^2$

Lower $|t|$ are dominated by fluctuations on larger length scales

Predictions for the EIC: Slope of incoherent cross section

H. Mäntysaari, B. Schenke, Phys. Rev. C101, 015203 (2020)

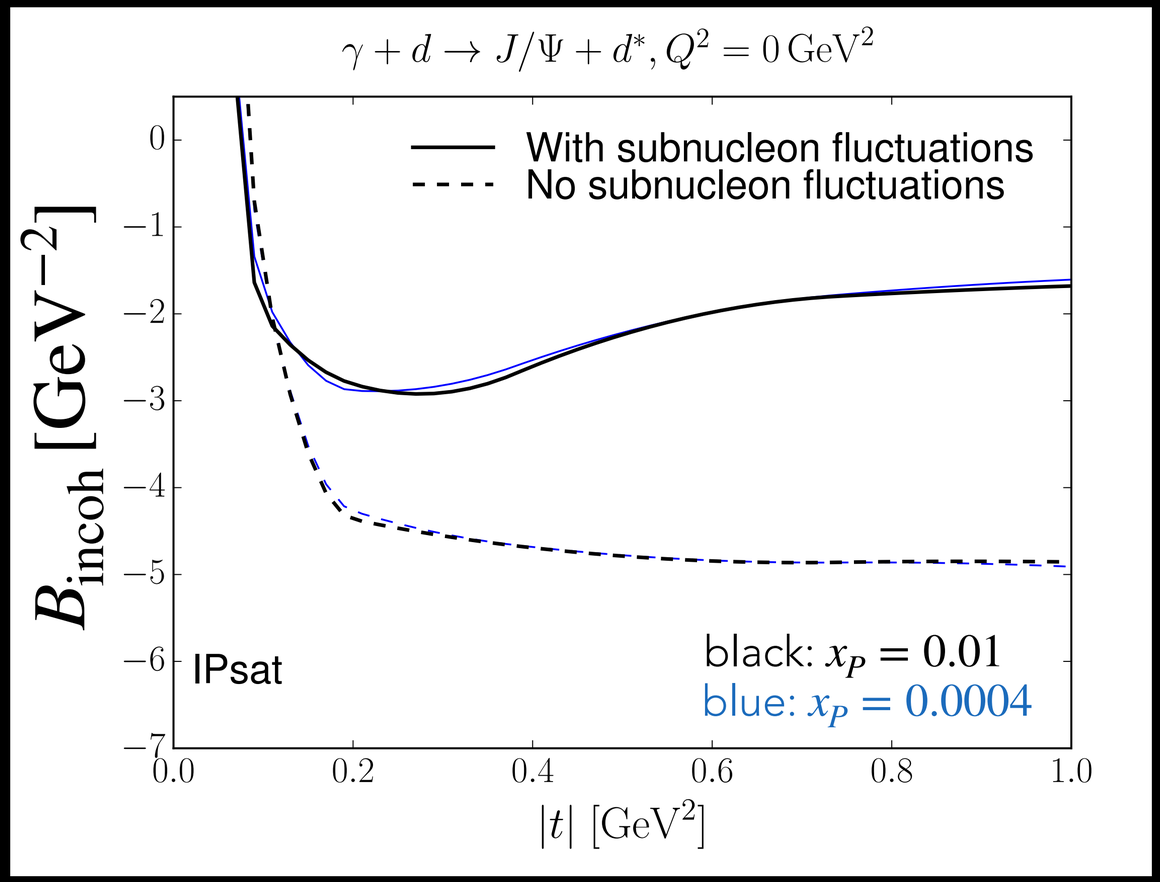

IPSat

Size of fluctuating object controls fall-off of the incoherent xsec $\sim e^{-B_{\mathrm{incoh}}|t|}$

see T. Lappi and H. Mäntysaari, Phys. Rev. C83 (2011) 065202

Predictions for the EIC: Slope of incoherent cross section

H. Mäntysaari, B. Schenke, Phys. Rev. C101, 015203 (2020)

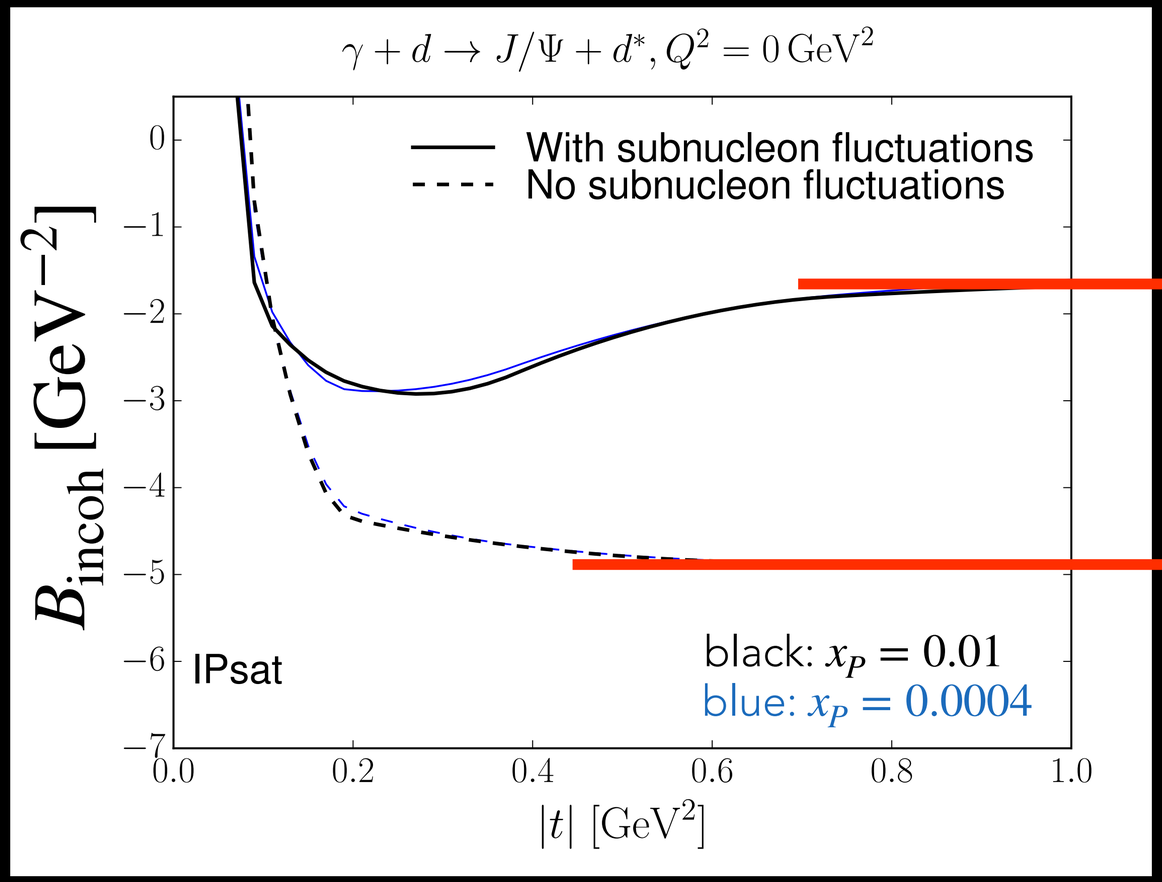

IPSat

hot spot scale $B_q = 1\,\mathrm{GeV}^{-2}$

nucleon scale $B_p = 4\,\mathrm{GeV}^{-2}$

Size of fluctuating object controls fall-off of the incoherent xsec $\sim e^{B_{\mathrm{incoh}}|t|}$

see T. Lappi and H. Mäntysaari, Phys. Rev. C83 (2011) 065202

Predictions for the EIC: Slope of incoherent cross section

H. Mäntysaari, B. Schenke, Phys. Rev. C101, 015203 (2020)

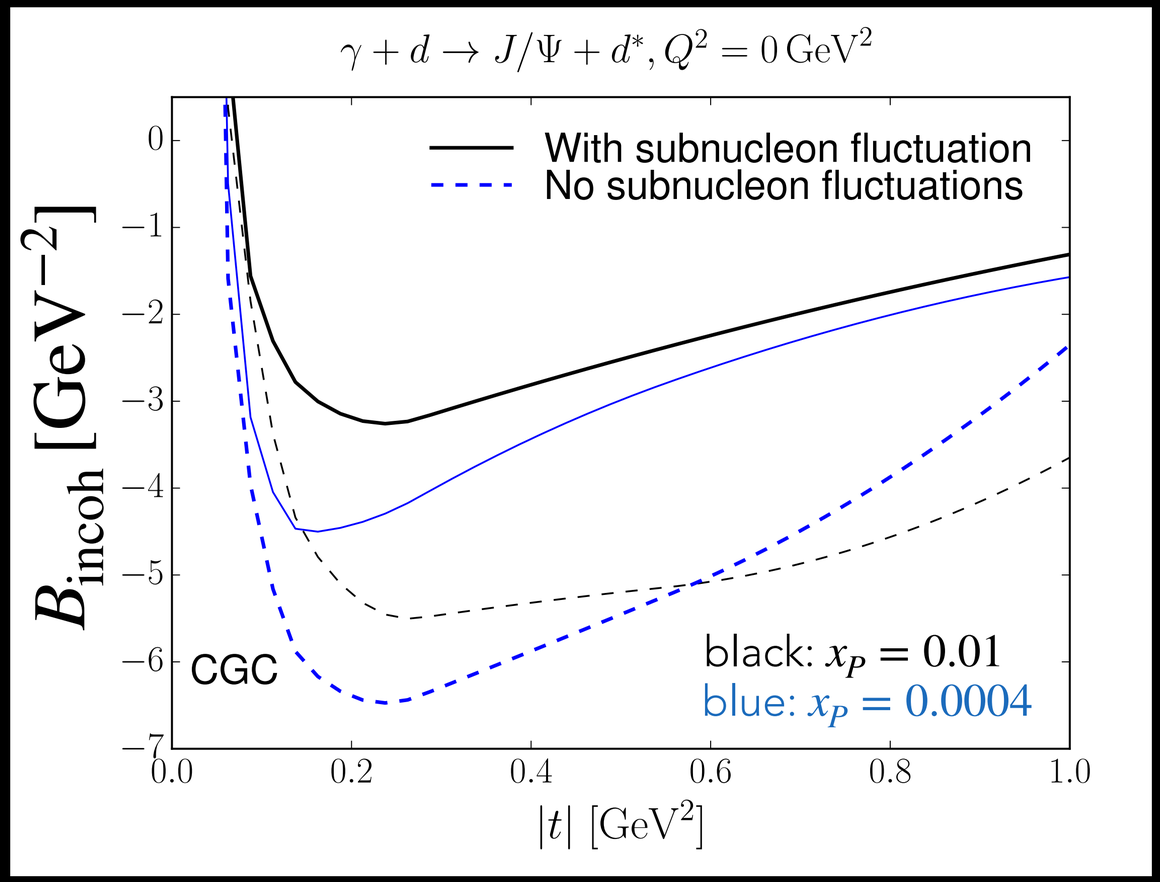

CGC

At $|t| \sim 0.2\,\mathrm{GeV}^2$ spectra become steeper with decreasing *x* (growth of the system and its fluctuating constituents)

Slopes are not constant at large $|t|$
Reason: Color charge fluctuations

At smaller *x* color charge fluctuations happen on shorter scale $\sim 1/Q_s$ (blue dashed line crosses black dashed line)

Predictions for the EIC: Cross sections for ^{3}He targets

H. Mäntysaari, B. Schenke, Phys. Rev. C101, 015203 (2020)

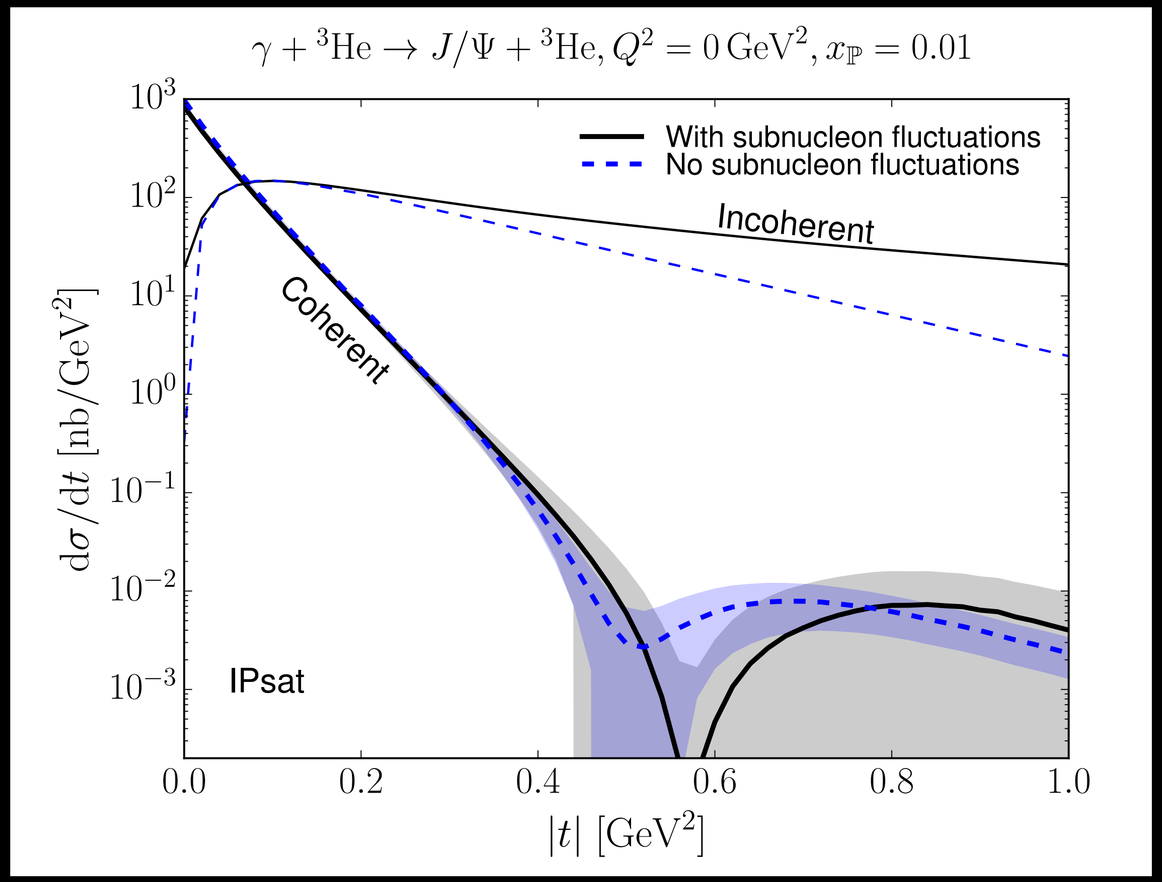

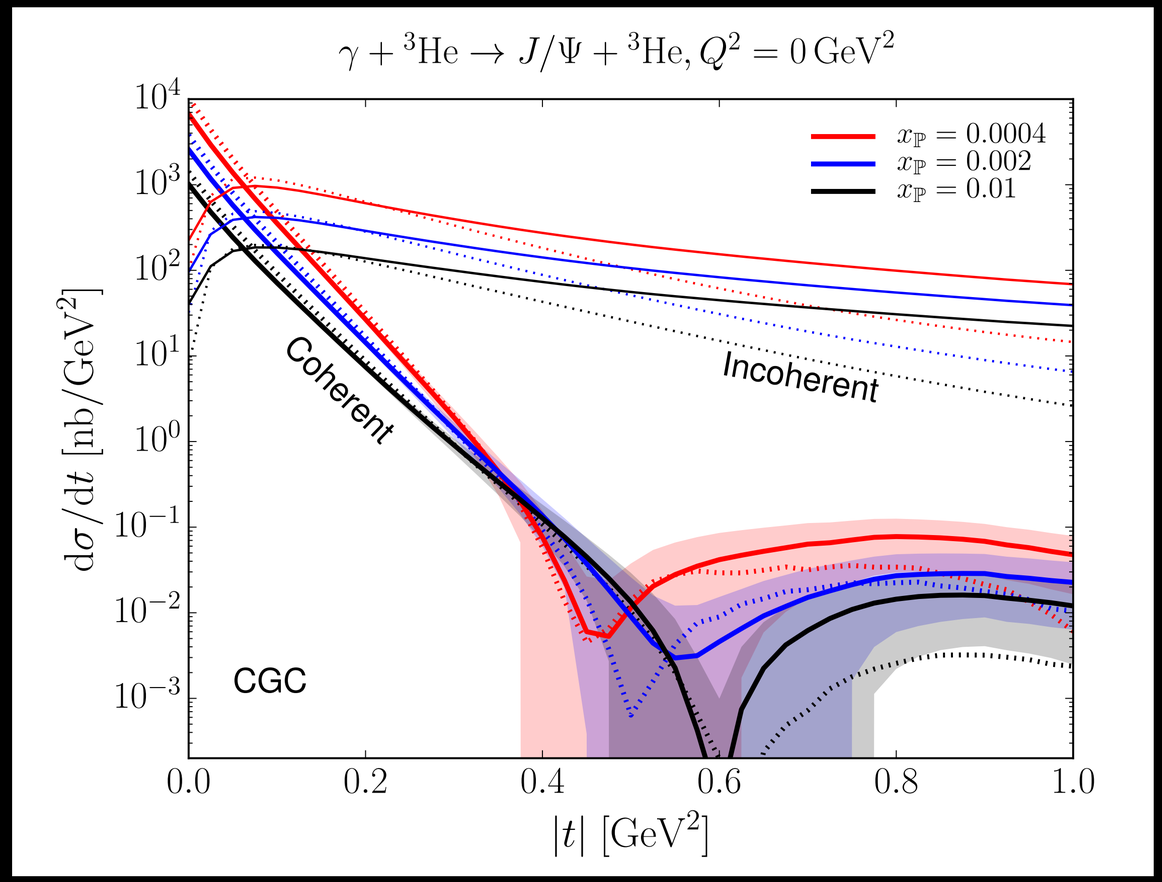

Predictions for the EIC: d vs. ^{3}He targets

H. Mäntysaari, B. Schenke, Phys. Rev. C101, 015203 (2020)

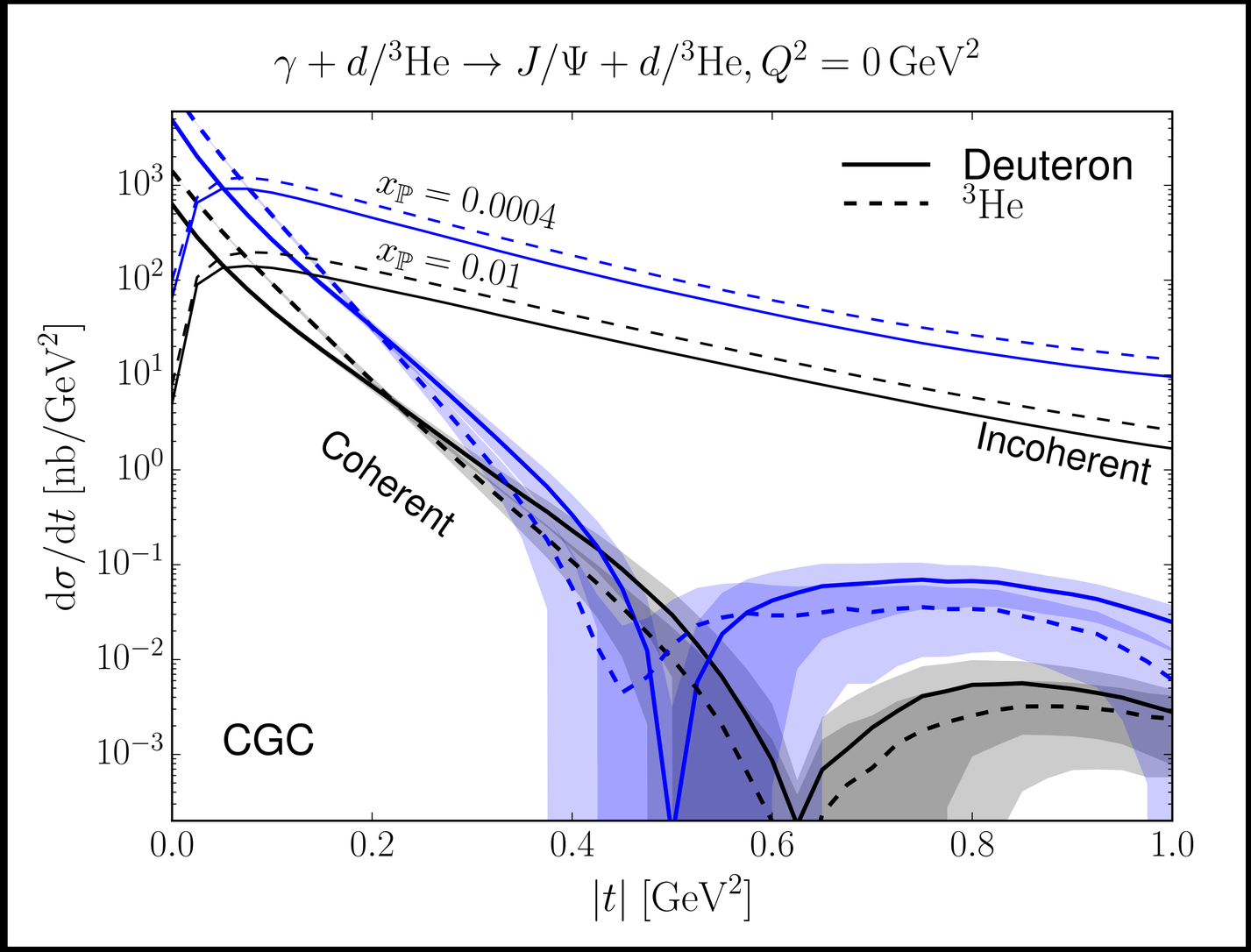

COLOR GLASS CONDENSATE

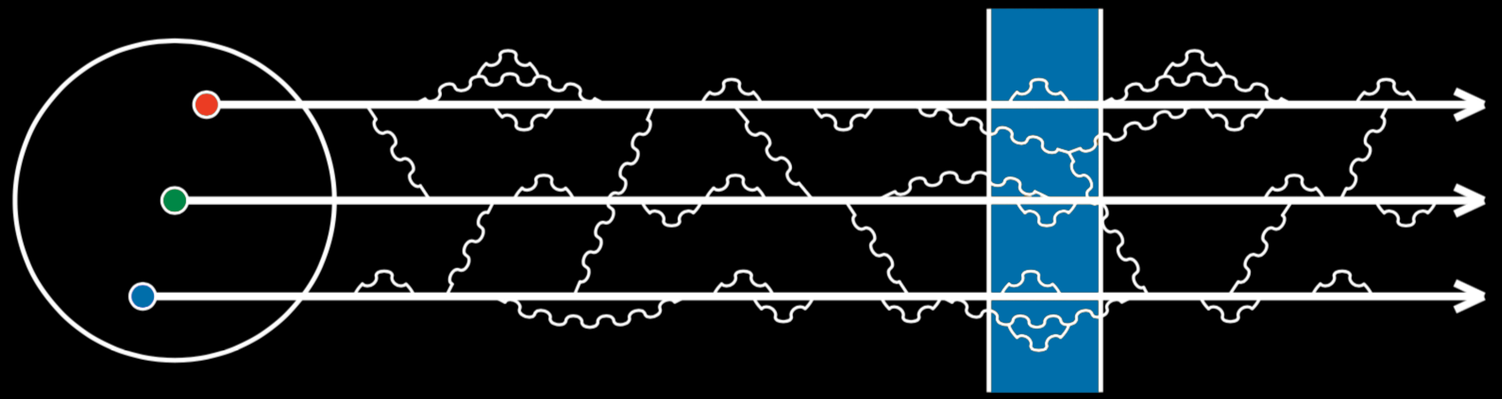

Figure from F. Gelis

Nucleon at rest:

- Complicated non-perturbative object
- Contains fluctuations at all scales smaller than its own size
- Only the fluctuations that are longer lived than the external probe participate in the interaction process
- The only role of short lived fluctuations is to renormalize the masses and couplings
- Interactions are very complicated if the constituents of the nucleon have a non trivial dynamics over time-scales comparable to those of the probe

COLOR GLASS CONDENSATE

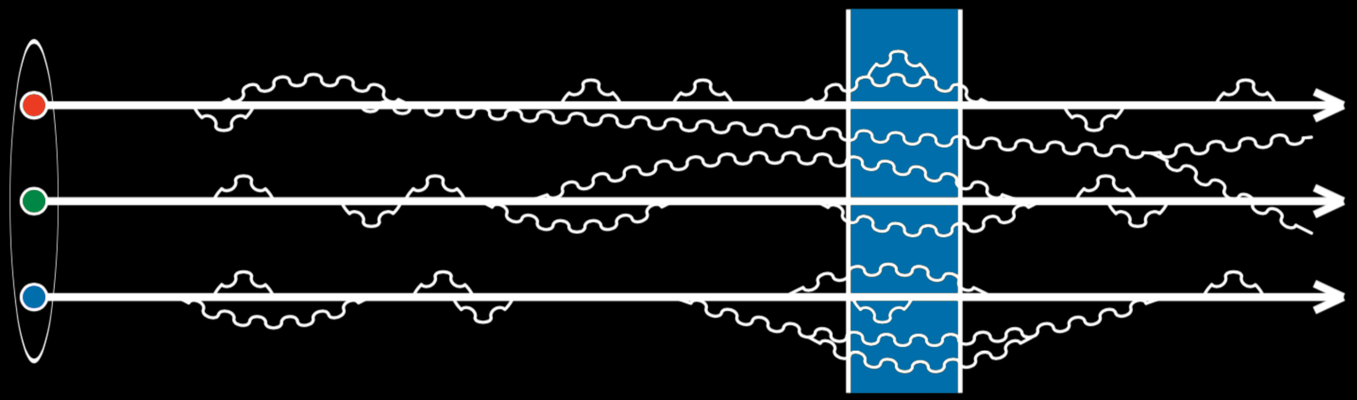

Figure from F. Gelis

Nucleon at high energy:

- Dilation of all internal time-scales of the nucleon
- Interactions among constituents now take place over time-scales longer than the characteristic time-scale of the probe → The constituents behave as if they were free
- Many fluctuations live long enough to be seen by the probe. Nucleon appears denser at high energy (contains more gluons)
- Pre-existing fluctuations are totally frozen over the time-scale of the probe, and act as static sources of new partons

Color Glass Condensate formalism

H. Mäntysaari, B. Schenke, Phys. Rev. C101, 015203 (2020)

From color charges we obtain Wilson lines at the initial $x_0 = 0.01$

$$V(\vec{x}) = P \exp\left(-ig \int dx^- \frac{\rho(x^-, \vec{x})}{\vec{\nabla}^2 + \tilde{m}^2} \right)$$

from solution of Yang-Mills equations, with regulator $\tilde{m} = 0.4\,\mathrm{GeV}$

Evolution in x uses the Langevin formulation of the JIMWLK equations

$$\frac{d}{dy} V(\vec{x}) = V(\vec{x})(it^a) \left[\int d^2z \varepsilon^{ab,i}_{\vec{x},\vec{z}} \xi_{\vec{z}}(y)^b_i + \sigma^a_{\vec{x}} \right]$$

with random noise ξ and coefficient $\varepsilon^{ab,i}_{\vec{x},\vec{z}} = \left(\frac{\alpha_s}{\pi}\right)^{\frac{1}{2}} K^i_{\vec{x}-\vec{z}} [1 - V^\dagger(\vec{x}) V(\vec{z})]^{ab}$

Color Glass Condensate formalism

H. Mäntysaari, B. Schenke, Phys. Rev. C101, 015203 (2020)

The kernel is given by $K^i_{\vec{x}} = \frac{x^i}{x^2}$

To regulate long distance tales we make the replacement

$$K^i_{\vec{x}} \to m|\vec{x}|K_1(m|\vec{x}|)\frac{x^i}{x^2}$$

Modified Bessel function K_1 suppresses contributions at distances $\gtrsim 1/m$

We use m=0.2 GeV